EXPERIMENT AND MODELLING OF EQUILIBRIUM BEACH PROFILE

WITH NET CROSS-SHORE SAND TRANSPORT

by

Annapurna Surya Sravani Mallavarapu, Nobushisa Kobayashi and Tingting Zhu

RESEARCH REPORT NO.CACR-18-02

July 2018

CENTER FOR APPLIED COASTAL RESEARCH
Ocean Engineering Laboratory
University of Delaware
Newark, Delaware 19716

ACKNOWLEDGMENT

TABLE OF CONTENTS

LIST OF TABLES

LIST OF FIGURES

ABSTRACT

Periodic beachfill placement and frequent overwash result in net offshore and onshore sand transport, respectively. Three tests consisting of fifty 400-s runs were conducted in a small-scale wave flume to examine the effect of net cross-shore sand transport on an equilibrium profile. The foreshore of an equilibrium profile with no net sand transport shifted seaward after periodic sand placement near the shoreline. Frequent sand overwash resulted in the landward shift of the shoreline. The profile changes among the three tests were relatively small and the shoreline shifts were less than 0.1 m. An analytical model for an equilibrium profile with net cross-shore sand transport is developed by approximating existing formulas for onshore bed load and offshore suspended sand transport in the inner surf zone. The model predicts the horizontal shift of the equilibrium profile under net cross-shore sand transport, which is the maximum at the shoreline and approaches zero at the closure depth. The model calibrated using the three tests are used to estimate the seaward shift of the shoreline on periodically-nourished beaches of prototype scale. The estimated shift is of the order of 1 m or less but will need to be verified using field data.

Chapter 1

INTRODUCTION

The concept of an equilibrium beach profile (Dean 1991) is expedient and has been adopted for the design of beachfills for beach nourishment (USACE 2003). The nourished beach maintained by periodic beachfill placement near the shoreline may become steeper to transport placed sand offshore. The present beachfill design does not account for the equilibrium profile modification caused by periodic beachfill placement. On the other hand, morphological changes of barrier islands caused by overwash during storms have been investigated in a number of studies [e.g., Jiménez et al. (2006); Rosati and Stone (2009)]. Frequent overwash may reduce the seaward beach slope to accommodate onshore sand transport near the shoreline. The beach profile modification caused by frequent overwash may not have been investigated previously.

The concept of an equilibrium profile has also been adopted for the prediction of shoreline response to sand sources, sinks, longshore sand transport gradients, and sea level rise [e.g., Dean and Houston (2016)]. The temporal change of sand volume in an active beach profile is expressed in terms of the temporal change of the cross-shore shoreline location of an equilibrium profile. This expression coupled with long-term shoreline change data was used to estimate an onshore transport rate of sand from beyond closure depth. The estimated rates were about 3 m^3/m per year during 1872-2007 along the 275-km Florida southwest coast (Dean and Houston 2016). Houston (2016) performed a similar analysis for the Florida east coast. The expression between

the sand volume and shoreline changes does not account for the equilibrium profile modification caused by sand sources and sinks.

The degree of the equilibrium beach profile modification caused by periodic beachfill placement or overwash may be difficult to quantify for natural beaches whose profiles change with water level and wave conditions. No reliable model exists to predict long-term beach profile evolution including periodic beachfill placement or frequent overwash (Kobayashi 2016). A laboratory experiment was conducted in this study to measure the beach profile changes caused by periodic beachfill placement and overwash. First, a quasi-equilibrium beach was established under constant water level and wave conditions. Second, sand was placed periodically near the shoreline of the equilibrium beach to produce a quasi-equilibrium profile with net offshore sand transport. Third, the still water level was increased to initiate wave overwash and produce a quasi-equilibrium profile with net onshore sand transport. The measured shoreline changes in the three tests are compared with the conventional method based on the cross-shore translation of an active profile caused by the source (periodic beachfill placement) and sink (overwash).

An equilibrium beach profile is regarded as a profile with no net cross-shore sediment transport rate (q_n). Kobayashi et al. (2008) proposed formulas for offshore suspended sediment transport rate q_s and onshore bed load transport rate q_b and derived the equilibrium profile equation of Dean (1991) for the case of $q_n = (q_s + q_b) = 0$ where onshore transport is positive in the following. Their model is extended analytically to equilibrium profiles with net offshore and onshore sediment transport rates.

2

The analytical model is compared with the measured quasi-equilibrium profiles in the small-scale experiment and used to estimate the offshore shoreline shift of a prototype beach under different nourishment rates. The analytical model is presented after the laboratory experiment and data analysis.

Chapter 2

EXPERIMENT

This Chapter provides an overview of the experiment which was conducted in University of Delaware wave flume located in basement of the Dupont Hall.

The experiment was conducted in a wave tank that is 30 m long, 2.5 m wide, and 1.5 m high. A dividing wall in the middle of the tank was installed to reduce the amount of sand used in the experiment, the water level change due to wave overtopping, and seiching development in the tank. Three tests listed in Table 2.1 were carried out in a 23-m long and 115-cm wide flume as shown in Figure 2.1. The sand beach in the flume consisted of well-sorted fine sand with a median diameter of 0.18 mm. The fall velocity, density, and porosity of the sand were 2.0 cm/s, 2.6 g/cm^3, and 0.4, respectively. This small-scale experiment was not intended to reproduce specific prototype conditions. This experimental setup and data collection were originally used by Figlus et al. (2011) to provide detailed measurements of overwash processes. The fine sand used in the experiment might be regarded as coarse sand at prototype scale. Both bed load and suspended load were discernible in the experiment.

A 400-s run of irregular wave train with a Texel, Marsen and Arsloe (TMA) spectral shape was generated by the paddle of the piston-type wave maker in a water depth of 88 cm for the first two (Z and N) tests with no wave overtopping and overwash. The spectral significant wave height and peak period were approximately 17 cm and 2.6 s. Nine wave gauges were placed in the flume. Wave gauges 1 to 8 (WG1-WG8) were used to measure the free surface elevation outside and inside the

surf zone and in the swash zone. The WG9 was used to measure the wave level in the basin after each run to measure the volume of overtopped water. The fluid velocities were measured by one acoustic Doppler velocimeter (ADV) sensor and two Vectrinos (Nortek, Rud, Norway) which were co-located at WG4, WG5, and WG6 (WG4 with 2D ADV and WG5-WG6 with Red and Blue Vectrinos) at an elevation of one-third of the local water depth. A vertical wall was located at the onshore coordinate $x = 19.9$ m with $x = 0$ at WG1. The vertical coordinate z was positive upward with $z = 0$ at the still water level (SWL). The still water level of tests N and P was 88 cm and that of P test was 92 cm. The elevation of the wall crest was 106 cm above the horizontal flume bottom. The wave overtopping rate q_o and sand overwash rate q_{bs} for the third (P) test in 92-cm water depth were measured by collecting overtopped water and sand in a water collection basin and a sand trap during each 400-s run.

Table 2.1:   Sequence of three tests with zero (Z), negative (N), and positive (P) net cross-shore sand transport

Test	Cross-shore sand transport	Water depth (cm)	Duration (s)
Z	Zero (equilibrium)	88	4,000
N	Negative (offshore)	88	8,000
P	Positive (onshore)	92	8,000

Acuity AR4000- LIR laser line scanner system was used to obtain accurate three dimensional profile data after each 10 runs (4,000 s) with constant SWL. The scanner mounted on a motorized cart recorded alongshore transects at 2-cm cross-shore intervals with a vertical error of about 1 mm after draining water in the tank.

The three-dimensional bathymetry data were averaged alongshore after confirmation of alongshore uniformity.
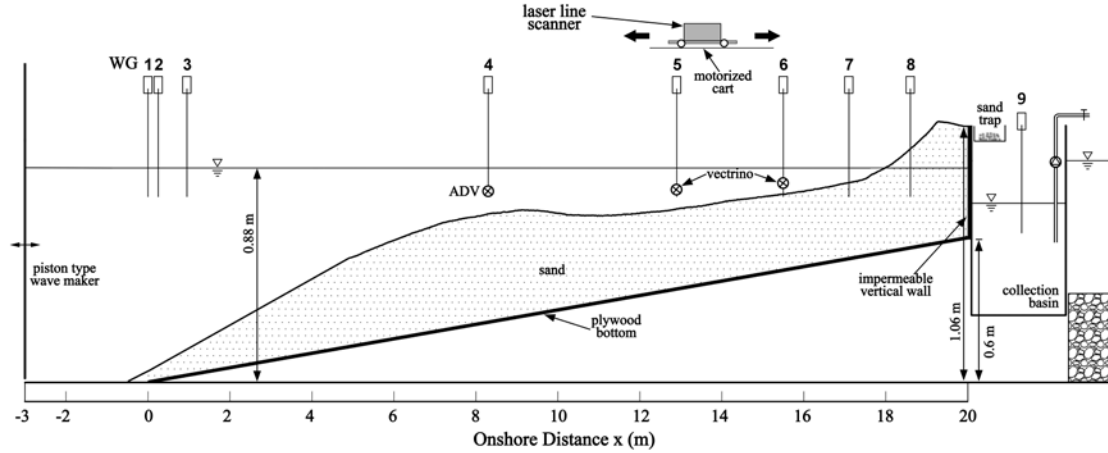
Figure 2.1:   Experimental setup at the start of Test Z with zero net sand transport rate

2.1   Three Tests

The initial profile of the Z test is depicted in Figure 2.1. Preliminary tests were conducted to finalize the Z, N, and P tests. The initial profile of Z0 was almost in equilibrium under the specified water level and wave conditions. The run number starting from run number 0 for the initial profile is affixed to the test name to indicate a specific run in each test. Ten 400-s runs were performed in the Z test. The profiles of Z5 and Z10 were measured after 5 and 10 runs. The measured profiles of Z0, Z5, and Z10 were compared to confirm the establishment of a quasi-equilibrium profile with elevation changes of a few millimetres.

The initial profile of the N test was the final profile of Z10. Sand was placed uniformly across the 115-cm wide flume near the shoreline of the initial profile of N0. The placed sand mass per unit width corresponded to the sand volume (no void) of

12 cm^3/cm. The placed sand was dispersed quickly during the first 400-s run. Additional four runs were generated and the beach profile of N5 was measured. The sand volume of 12 cm^3/cm was placed again and exposed to five runs and the beach profile of N10 was measured and compared with the profiles of N0 and N5. Since the profile changes were small, the placed sand volume was increased to 24 cm^3/cm and exposed to 10 runs. The beach profile of N20 was measured and compared with the profile of N10. The two profiles were very similar apart from the offshore shift of the foreshore slope of approximately 1/8 (vertical/horizontal). For the N test, the total placed sand volume per unit width was 48 cm^2 for the duration of 8,000 s. The average rate of the sand placement per unit width was 0.006 cm^2/s.

The initial profile of the P test was the final profile of N20. The SWL was raised by 4 cm and the water depth of 88 cm in Figure 2.1 increased to 92 cm in the P test. The 4-cm SWL increase was selected on the basis of a preliminary test in which the measured sand overwash rate q_{bs} was about 0.006 cm^2/s. The beach profiles of P5, P10, and P20 were measured during 20 runs in the P test. The wave overtopping rate q_o and sand overwash rate q_{bs} were measured for each run.

Chapter 3

DATA ANALYSIS

Analysed data are summarized in the following. Detailed data are presented in the Appendix.

3.1 Free Surface and Velocity Statistics

The time series from Wave Gauges WG1 – WG3 located at x = 0.0, 0.25, and 0.95 m for each run were used to separate incident and reflected waves at the location x = 0 of WG1. The spectral significant wave height H_{mo} and peak period T_p of incident waves were approximately 17 cm and 2.6 s. The reflection coefficient, defined as the ratio between the values of H_{mo} for the reflected and incident waves, was approximately 0.14. The measured time series of the free surface elevation η above the SWL and velocities for the 50 runs were analysed to examine the cross-shore wave transformation in the Z, N, and P tests. The analysed data for the 10 runs of Z1-Z10, N11-N20, P11-P20 are presented in Figure 3.1, Figure 3.2 and Figure 3.3 respectively. The variability among the 10 runs resulted from the slight bottom profile change, errors of the measurements and wave reproduction.

The measured values of the mean $\bar{\eta}$ were slightly negative (wave set down) at WG1 – WG3 outside the surf zone and at WG4 (x = 8.3 m) in the outer surf zone where large waves broke. The relatively steep bottom slope of about 1/10 in the offshore zone of x < 5 m in Figure 2.1 was necessary because of the limited flume length. A small bar below WG4 may have been caused by breaking of large waves.

The values of $\bar{\eta}$ were positive (wave setup) at WG5 – WG7 at x = 12.9, 15.5, and 17.1 m in the inner surf zone. The value $\bar{\eta}$ of WG8 at x = 18.6 m in the swash zone is the sum of the bottom elevation (10.1 – 10.2 cm for Test P) above the SWL and the mean depth $\bar{h}$ (1.5 – 2.3 cm for Test P). The averaging for WG8 buried partially in the sand was performed for the wet duration. The wet probability P_w was defined as the ratio between the wet and total duration. P_w = 1.0 at WG1 – WG7 and P_w = 0.60 – 0.64 at WG8 in Figure 3.3. The standard deviation (SD) σ_η of the free surface elevation was related to the wave height decay caused by irregular wave breaking where the local significant wave height H_{mo} was defined as $H_{mo} = 4\,\sigma_\eta$. Wave shoaling from x = 0.0 – 0.95 m to x = 8.3 m was not discernible in Figures 3.1, 3.2 and 3.3. Wave breaking reduced σ_η noticeably from x = 8.3 m to x = 12.9 m and gradually in the inner surf zone (x = 12.9 – 17.1 m). Waves broke near the toe of the foreshore slope and ran up in the swash zone (x = 18.6 m).

The measured alongshore and vertical velocities were small in comparison with the cross-shore velocity U. The mean velocity $\bar{U}$ was negative (undertow) because of the wave-induced offshore return current. The offshore current decreased from the outer surf zone (x= 8.3 m) to the inner surf zone (x = 12.9 – 15.5 m). The standard deviation σ_U of the oscillatory component of the velocity U also decreased landward.
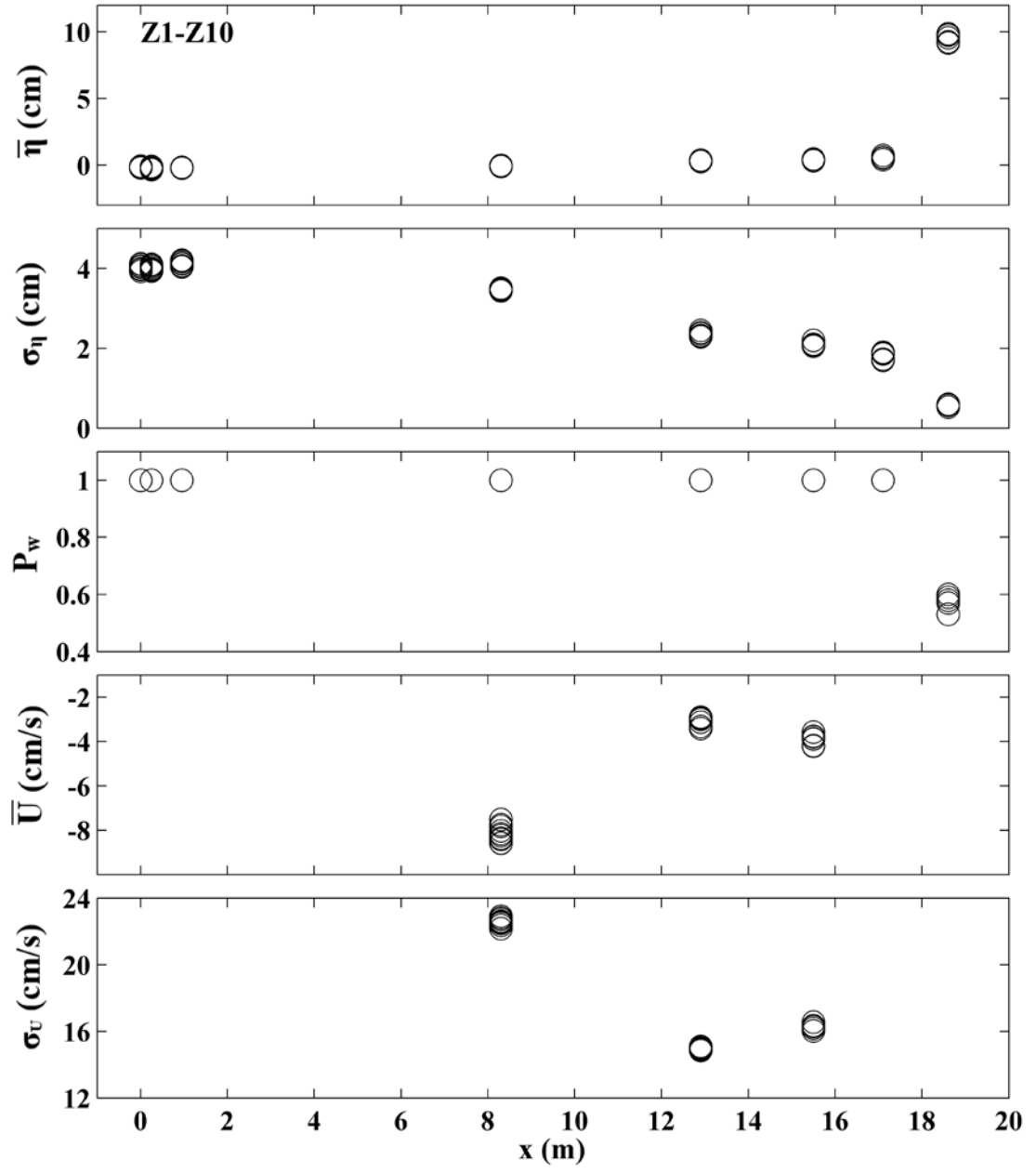
Figure 3.1: Mean and standard deviation of free surface elevation η and horizontal velocity U together with wet probability P_w for 10 runs during time t = 0 – 4,000 s in Test Z
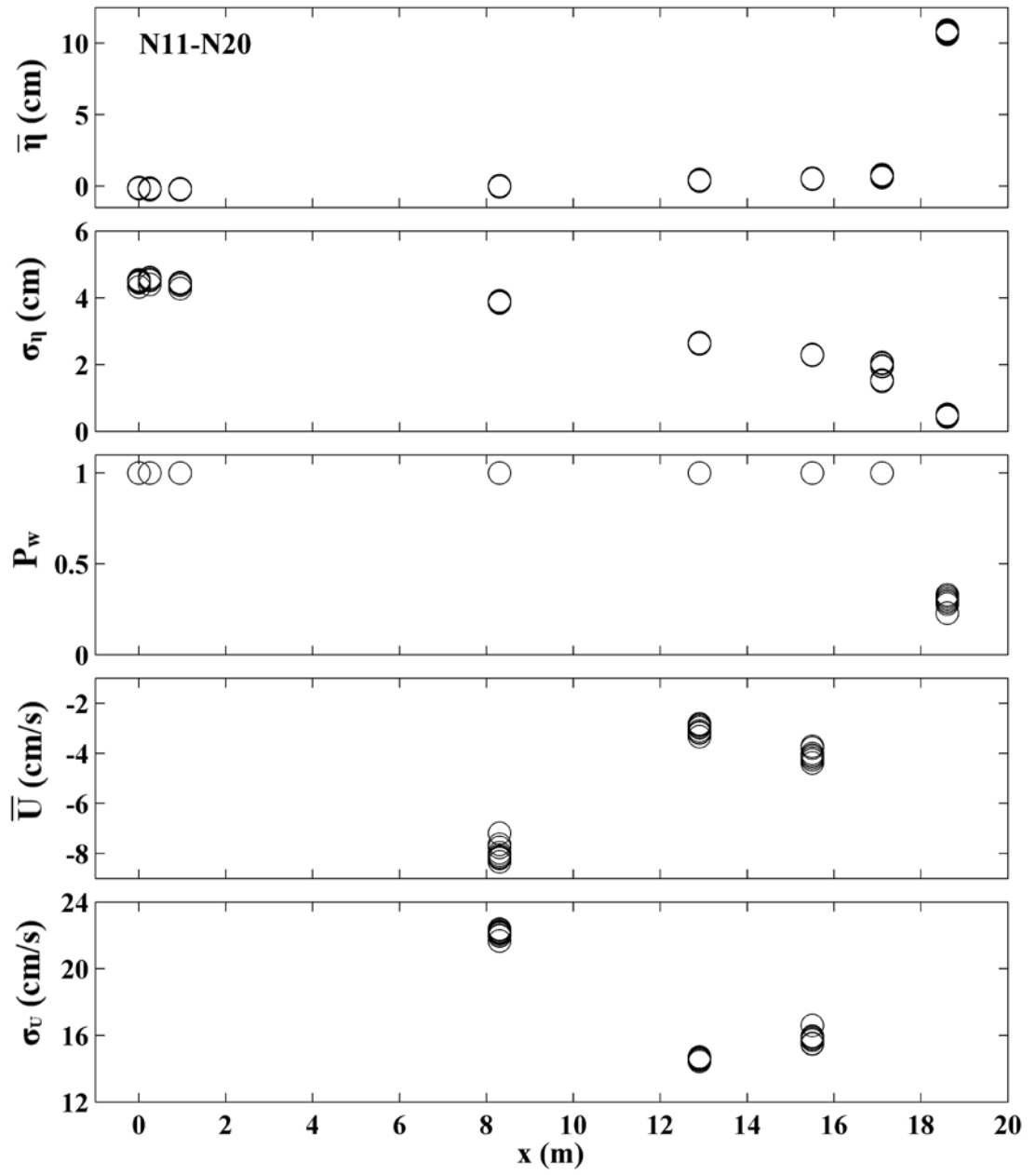
Figure 3.2: Mean and standard deviation of free surface elevation η and horizontal velocity U together with wet probability P_w for 10 runs during time t = 4,000 – 8,000 s in Test N

11
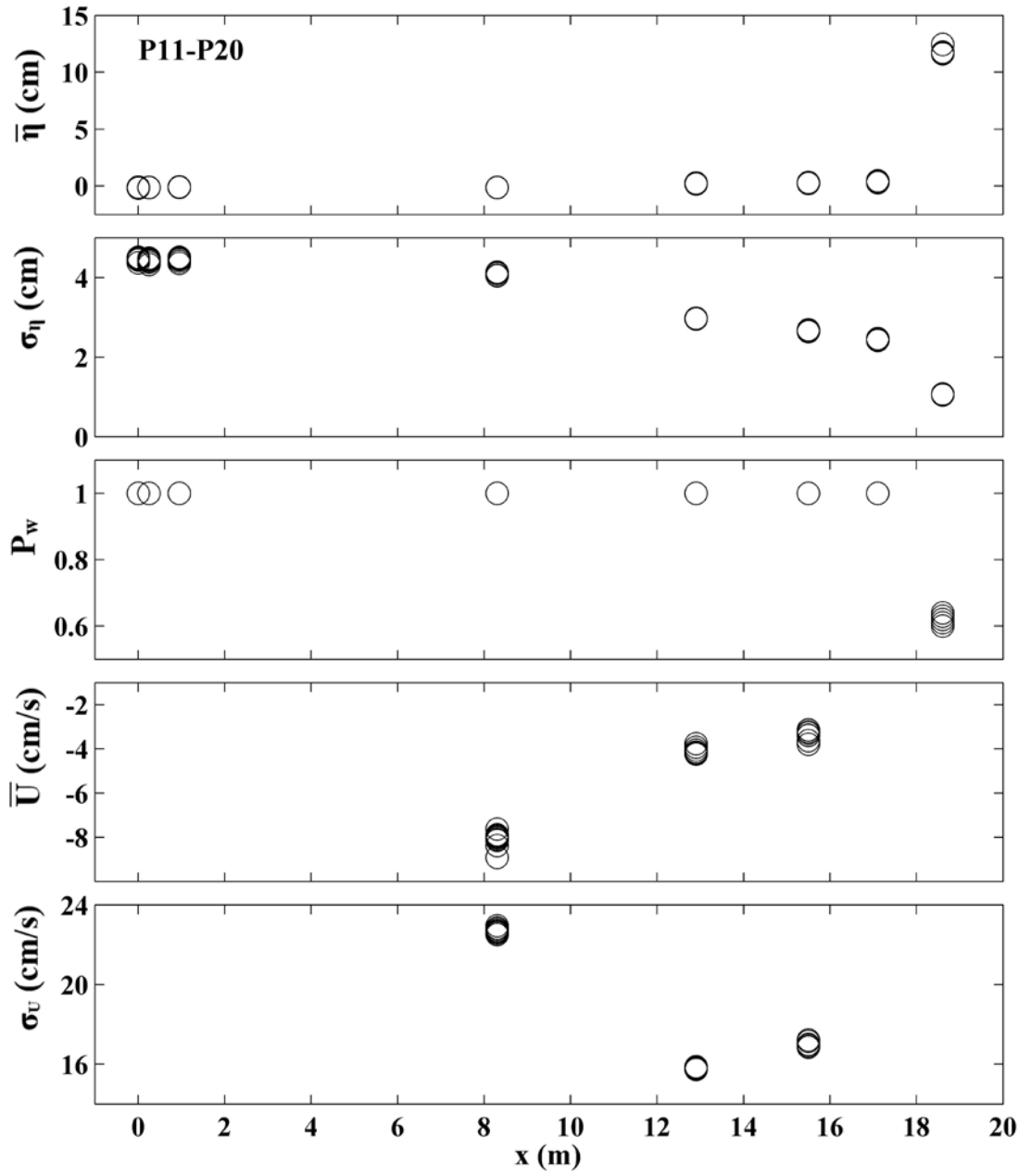
Figure 3.3:   Mean and standard deviation of free surface elevation η and horizontal velocity U together with wet probability P_w for 10 runs during time t = 4,000 – 8,000 s in Test P

3.2 Beach Profile Evolution

The measured beach profiles in each test were plotted together to examine the degree of the profile changes. The vertical profile changes during the 5 or 10 runs were a few millimeters in the zone of $x < 11$ m and up to 1 cm in the zone of $x > 17$ m. Figure 3.4 shows the initial and final profiles of the Z, N, and P tests in the zone of $x > 11$ m. The intermediate profiles of Z5, N5, N10, P5, and P10 between the initial and final profiles are not plotted in Figure 3.4 for clarity. During the Z test, a step-like feature developed at the lower limit of wave downrush on the foreshore slope, and slight erosion and accretion occurred seaward and landward of the step, respectively. The SWL shoreline of the profile Z0 shifted seaward by 3.6 cm (4.1 cm) for the profile Z5 (Z10). The profile change from Z5 to Z10 was less than 5 mm and the profile Z10 was regarded as quasi-equilibrium.

For the N test with sand placement near the shoreline, the foreshore slope and step translated seaward and the beach profile in the zone of $x < 17$ m changed little. The SWL shoreline of the profile N0 shifted seaward by 3.7, 4.1, and 9.0 cm for N5, N10, and N20, respectively. For the P test with wave overtopping and sand overwash, erosion (accretion) occurred on the lower (upper) part of the foreshore and its slope became slightly steeper. The step at the toe of the foreshore migrated onshore as the foreshore crest became higher by 1 cm. The SWL shoreline of the profile P0 shifted landward by 7.3, 7.0, and 8.1 cm for P5, P10, and P20. The conservation of sand volume is examined in the next section.

For the P test, the volumes of water and sand transported over the vertical wall in Figure 2.1 were used to obtain the water overtopping rate q_o and sand overwash rate q_{bs} per unit width averaged over each 400-s run. Figure 3.5 shows the temporal variations of q_o and q_{bs} for the 20 runs. The average rates are plotted at

time t (t=0 at the start of the test) corresponding to the end of each run. Both q_o and q_{bs} decreased with time t as the foreshore crest became higher. The ratio of q_o/q_{bs} did not change much and was about 0.035. The overwashed sand volume per unit width was 27 cm^2 for the duration of 8,000 s.
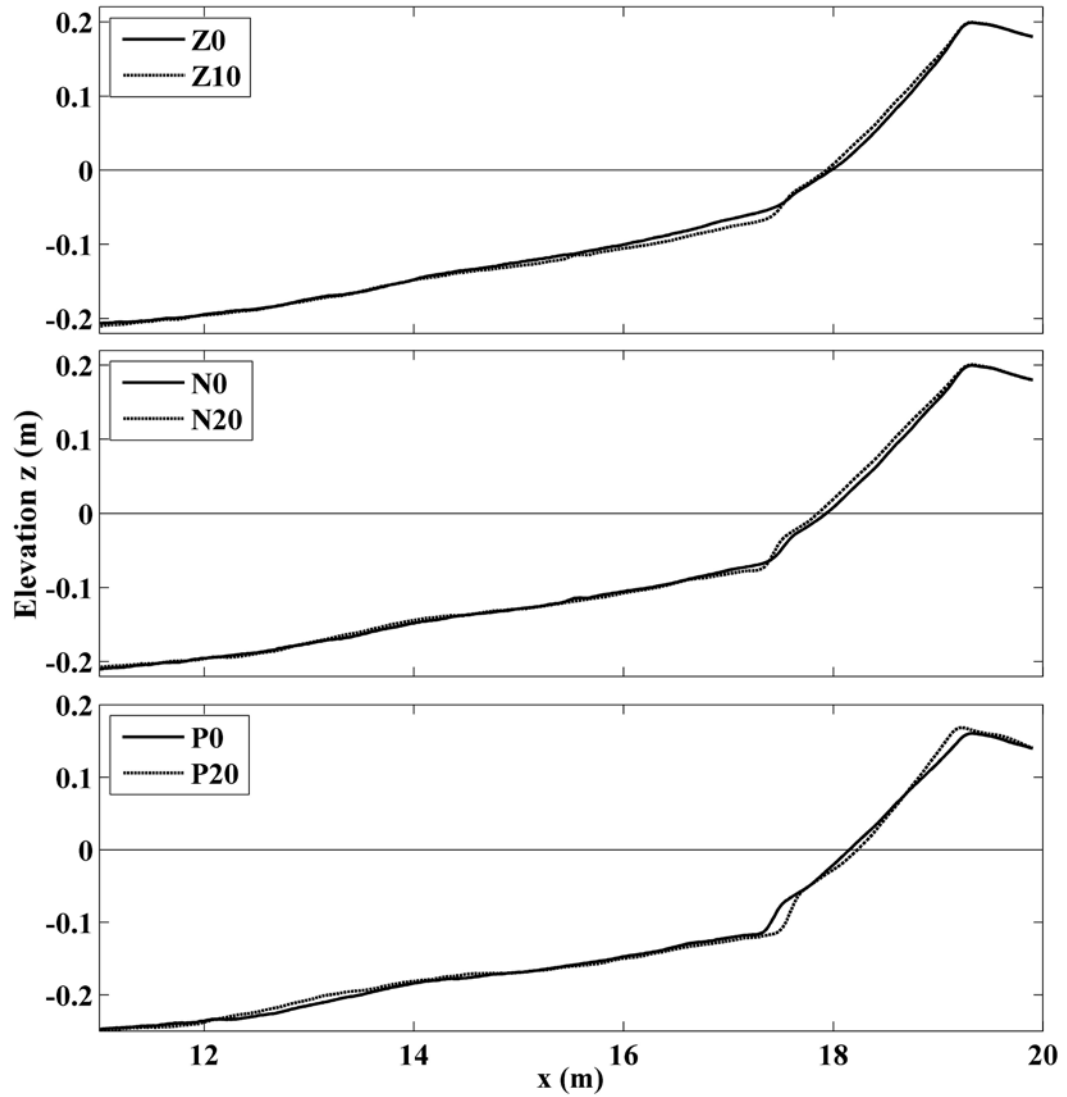
Figure 3.4:   Initial and final beach profiles for Tests Z, N and P
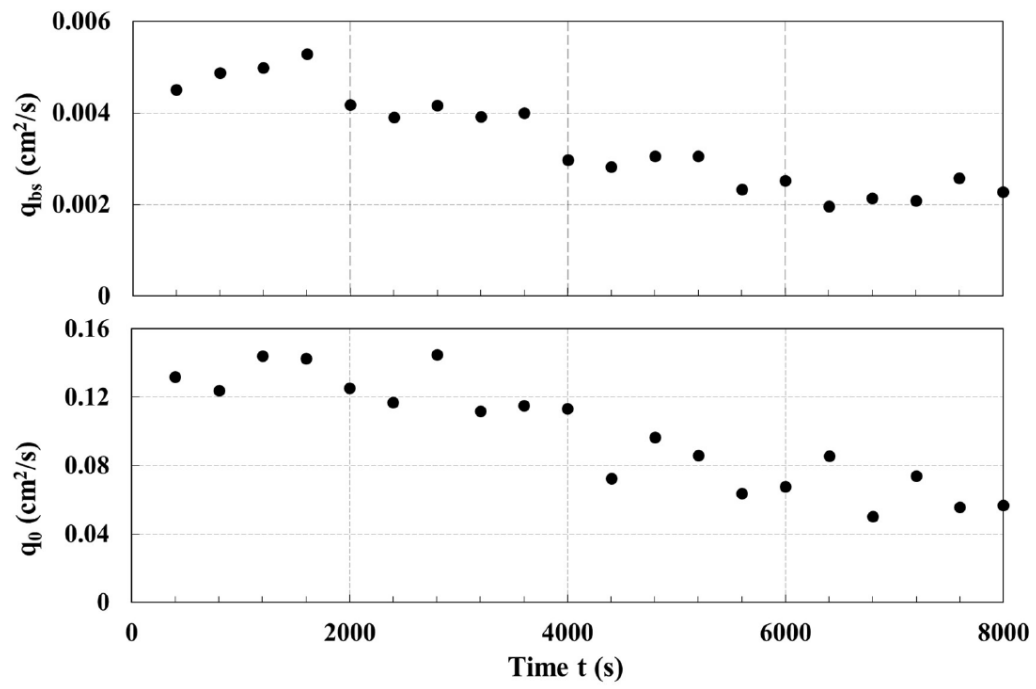
Figure 3.5:   Temporal variations of wave overtopping rate q_o and sand overwash rate q_{bs} for Test P

Chapter 4

CONVENTIONAL SHORELINE TRANSLATION MODEL

In this chapter a conventional shoreline translation model has been developed and is compared to the data obtained from the experiment.

4.1 Comparison of Data with Conventional Method

The shoreline shifts in the N and P tests were caused by the periodic sand placement (source) and overwash (sink). An equation with terms representing all phenomena affecting shoreline change including Bruun-rule recession, onshore sand transport, sand sources and sinks, and longshore transport gradients was already established [e.g., Dean and Houston (2016)]. The measured shoreline shifts are compared with the conventional method based on the conservation of sand volume and active profile translation. The relationship between the SWL shoreline located at $x = x_o$ and the net cross-shore sand transport rate q_n is expressed as

$$(B + d_c)\frac{dx_0}{dt} = \frac{q_n}{1 - n_p} \tag{4.1}$$

where, t = time; B = berm height above the SWL; d_c = closure depth; n_p = sand porosity ($n_p = 0.4$ in this experiment). The net rate q_n is positive onshore and the shoreline location x_o shifts landward for $q_n > 0$ and seaward for $q_n < 0$. An equilibrium profile is assumed in Equation (4.1) because x_o is constant for $q_n = 0$. Equation (4.1) cannot explain the shoreline shift in the Z test with $q_n = 0$.
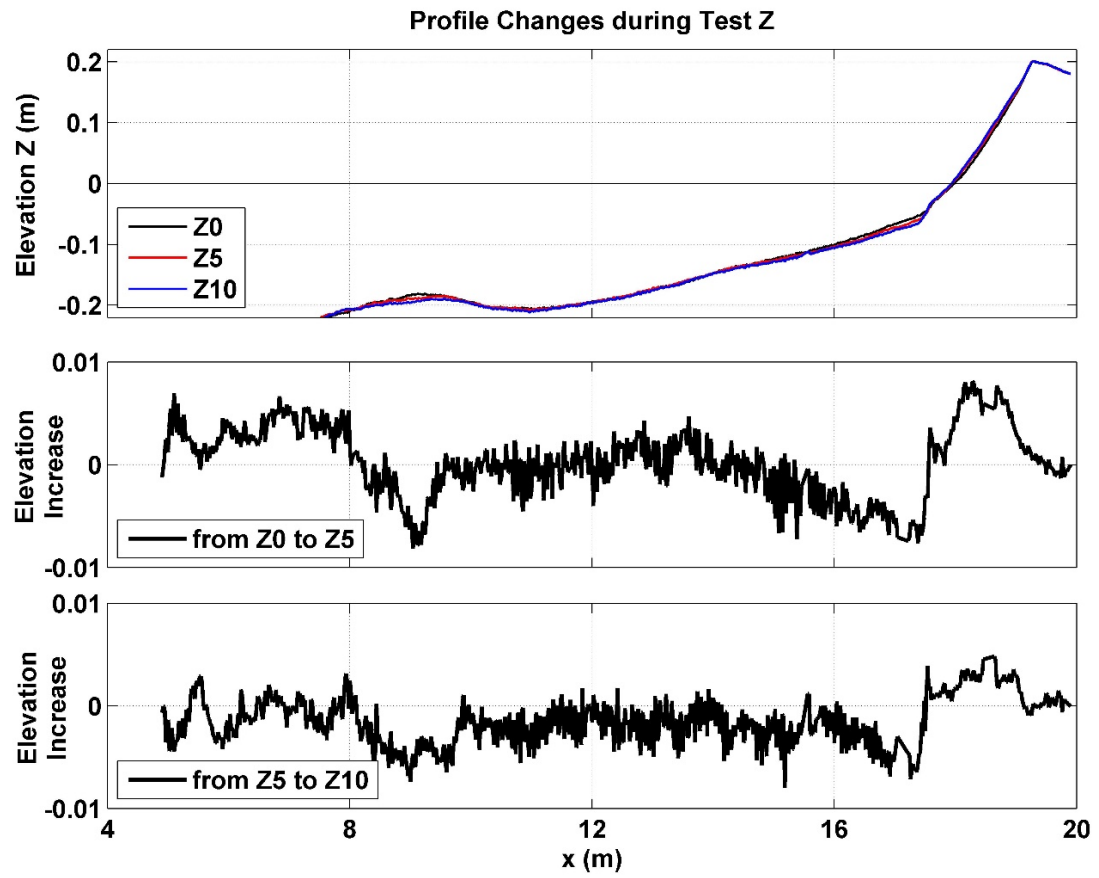
Figure 4.1: Zero (Z) net cross-shore sediment transport test with 10 runs and elevation increase from Z0 to Z5 and Z5 to Z10
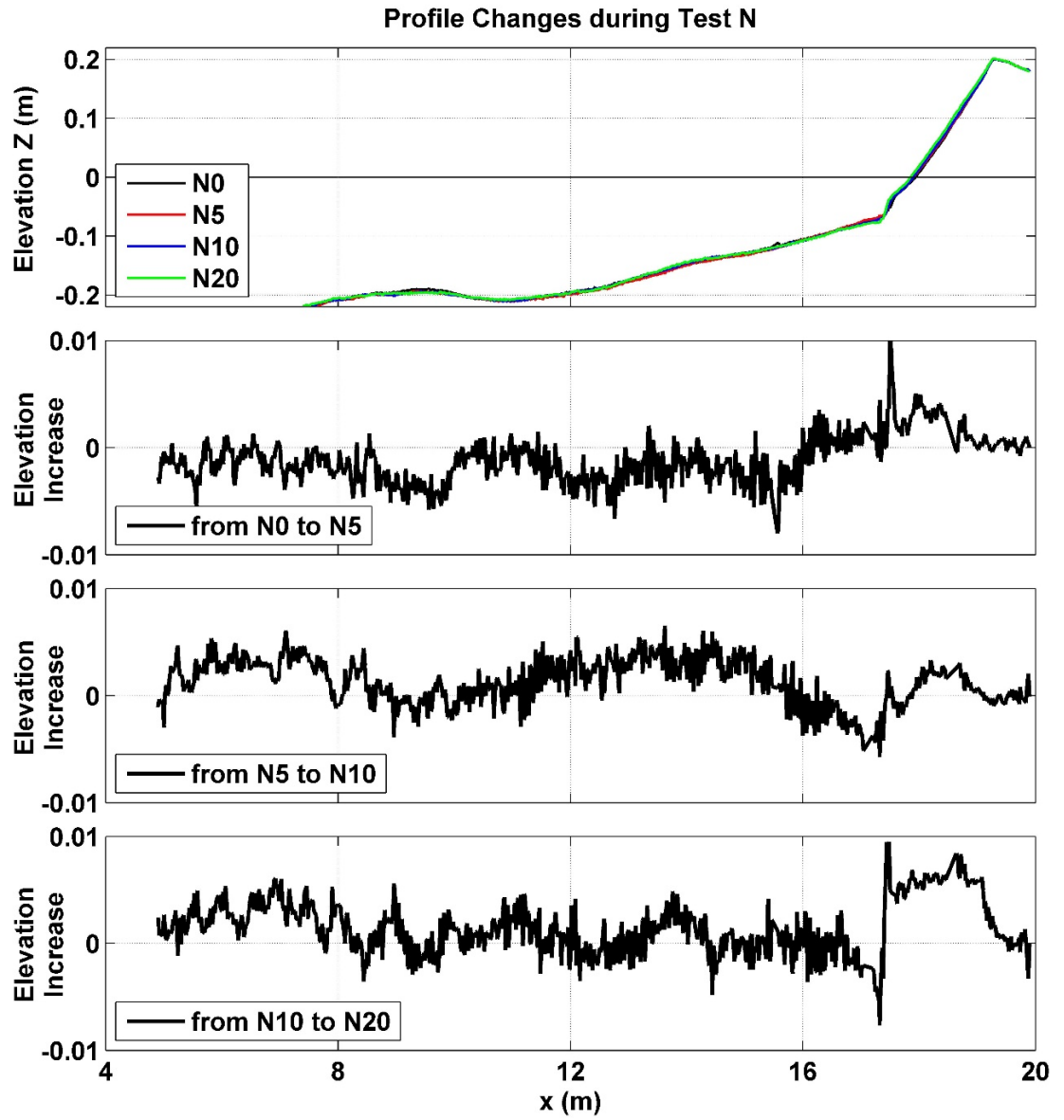
Figure 4.2: Negative (N) net cross-shore sediment transport test with 20 runs and elevation increase from N0 to N5, N5 to N10 and N10 to N20
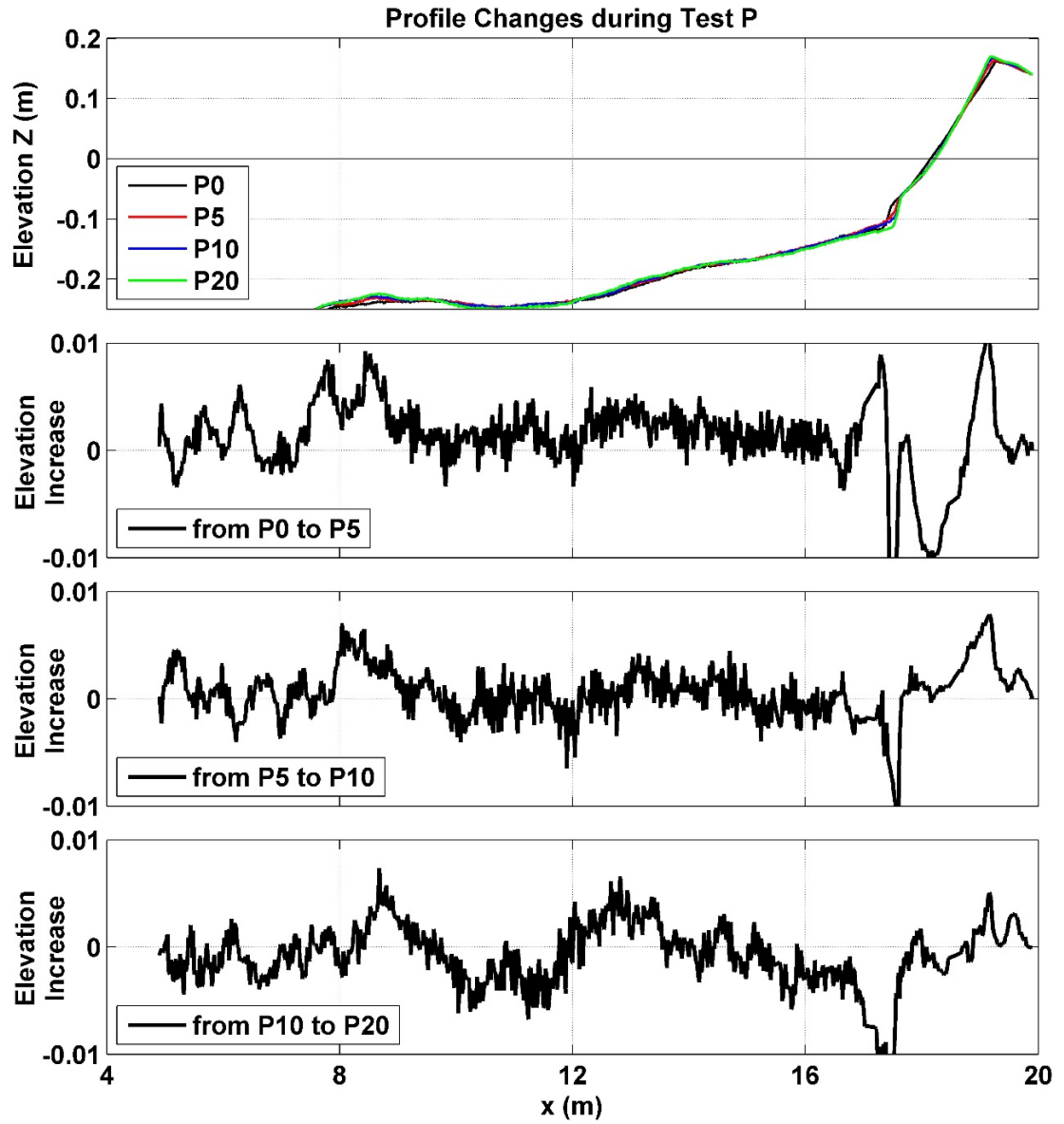
Figure 4.3: Positive (P) net cross-shore sediment transport test with 20 runs and elevation increase from P0 to P5, P5 to P10 and P10 to P20

Figure 4.1, Figure 4.2 and Figure 4.3 are used to estimate the berm height B and the closure depth d_c for the Z, N and P tests, respectively and the degree of profile equilibrium in each test. The foreshore crest height above the SWL is used to estimate

B = 0.20 m for the Z and N tests and B =0.17 m for the P test. The cross-shore location x_c = 11.7 m of the minimum (1 mm) profile change near the seaward edge of the inner surf zone is assumed to correspond to the closure location where d_c = 0.20 m for the Z and N tests and d_c=0.24 m for the P test. The estimated depth of closure and berm height are tabulated in Table 4.1.

Table 4.1:   Closure depth (d_c) and Berm Height (B) for Tests Z, N, and P

Test	d_c (m)	B (m)	(B+ d_c)(m)
Z	0.20	0.20	0.40
N	0.20	0.20	0.40
P	0.24	0.17	0.41

The minimum profile change implies almost zero gradient of the net cross-shore sand transport rate at the closure depth. The active profile height (B+d_c) is approximately 0.4 m. The net rate q_n for the N test is assumed to be constant and given by q_n= -0.006 cm^2/s. The net rate q_n for the P test is taken as the sand overwash rate q_{bs} in Figure 3.5.

4.2   Computed and Measured Shoreline Displacement

Integration of Equation (4.1) yields the shoreline displacement Δx_o defined as

Δx_o (t) = [x_o (t) - x_o (t=0)]

$$\Delta x_o(t) = \frac{Q_n(t)}{(B+d_c)(1-n_p)} \; ; Q_n(t) = \int_0^t q_n \, dt \qquad (4.2)$$

where, Q_n = cumulative sand volume per unit width which is added (negative) or removed (positive) from the active profile. The temporal variations of Q_n for the N

test and Q_n for the P test are shown in Figure 4.4. The placed sand volume in the N test was selected so that the absolute values of Q_n for the N and P tests would become similar. However, the reduction of q_{bs} caused by the foreshore crest accretion decreased Q_n in the P test.
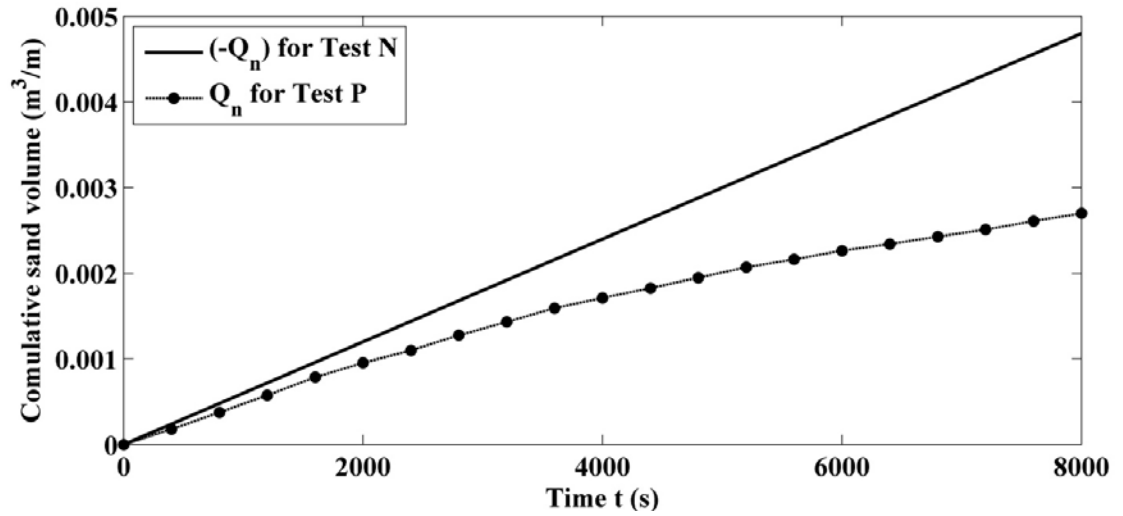
Figure 4.4:   Time series of cumulative sand volume per unit width for Tests N and P

Figure 4.5 compares the measured and computed shoreline displacements, which are negative (seaward) for the N test and positive (landward) for the P test. The computed displacement is too small partly because the entire active profile did not adjust itself within the test duration of 8,000 s. The profile adjustment was slower than expected. Using the measured value of Δx_o at $t = 8,000$ s in Equation (4.2), the calculated value of $(B + d_c)$ is 9 cm for the N test and 6 cm for the P test.

Table 4.2:   Measured location x_0 (m) at elevation $z = 0$ m for Test Z in 88-cm water depth and computed shoreline displacement Δx_0 (cm)

Time t(s)	0	2000	4000
x_0 (m)	17.981	17.945	17.940
Measured Δx_0 (cm)	0	-3.6	-4.1
Computed Δx_0 (cm)	0	0	0

Table 4.3:   Measured location x_0 (m) at elevation $z = 0$ m for Test N in 88-cm water depth and computed shoreline displacement Δx_0 (cm)

Time t(s)	0	2000	4000	8000
x_0 (m)	17.940	17.903	17.899	17.850
Measured Δx_0 (cm)	0	-3.7	-4.1	-9.0
Computed Δx_0 (cm)	0	-0.5	-1.0	-2.0

Table 4.4:   Measured location x_0 (m) at elevation $z = 0$ m for Test P in 92-cm water depth and computed shoreline displacement Δx_0 (cm)

Time t(s)	0	2000	4000	8000
x_0 (m)	18.152	18.225	18.222	18.233
Measured Δx_0 (cm)	0	7.3	7.0	8.1
Computed Δx_0 (cm)	0	0.4	0.7	1.1

The measured and computed shoreline displacements for the Z, N and P tests are tabulated in Table 4.2, Table 4.3 and Table 4.4 respectively. For the N test, the initial profile of N0 was quasi-equilibrium under the specified water level and waves. The profile adjustment was caused by the periodic sand placement near the shoreline. The placed sand was distributed on the foreshore and step in the zone of x > 17 m in Figure 3.4. The accreted area was 167 cm^2 and the eroded area in the vicinity of the

22

step was 59 cm^2. The difference was 108 cm^2 in comparison to the placed sand area of 80 cm^2 including void. For the P test, the initial profile of P0 was not in equilibrium with the SWL raised by 4 cm. The profile adjustment to the raised SWL was included in the measured shoreline displacement. The step migrated landward and the eroded area in the vicinity of the step was 186 cm^2. The deposited area on the upper foreshore was 91 cm^2 and the overwashed sand volume per unit width was 45 cm^2 including void. The unaccounted area of 50 cm^2 (e.g., 1 mm over a distance of 5 m) indicates the amplified error in the sand volume conservation resulting from the profile measurement error.
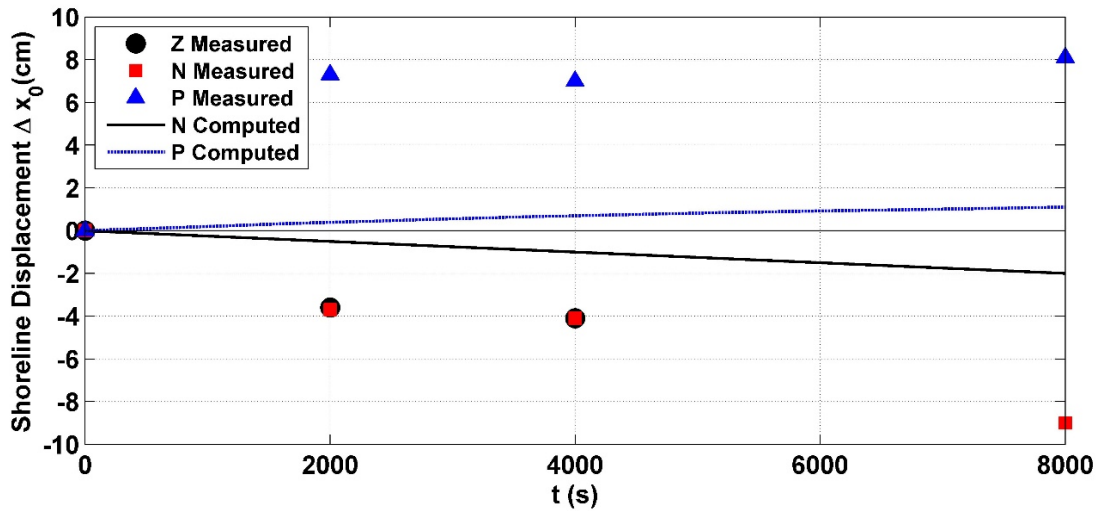
Figure 4.5: Measured and computed shoreline displacement Δx_o which is negative for Test N and positive for Test P

Chapter 5

NEW EQUILIBRIUM PROFILE MODEL

Some key features of a beach profile include (1) a concave upward profile, (2) smaller and larger sand diameters are associated with milder and steeper slopes respectively and (3) an approximately planar slope near the shoreline.

5.1   Background

The continuity equation of bottom sand for an equilibrium (no temporary change) profile under the assumption of alongshore uniformity requires no cross-shore gradient of the net cross-shore sand transport rate q_n. This requirement yields

$$q_b + q_s = q_n \; ; q_n = constant \tag{5.1}$$

where, q_b and q_s = cross-shore bed load and suspended load transport rates per unit width, respectively.   Kobayashi et al. (2008) approximated their formulas for the onshore rate q_b and the offshore rate q_s to derive the equilibrium profile popularized by Dean (1991). The approximations, which may be reasonable in the inner surf zone, included the assumptions of shallow water, negligible wave setup, and constant ratio σ_η/h with h = still water depth in the inner surf zone where h is assumed to decrease landward monotonically. This study does not address the issue of q_n outside the inner surf zone.

5.2 Formulation of Analytical Solution

The approximate expressions of q_b and q_s can be shown to be written using $y = h^{1.5}$

$$q_b = \alpha y \;\; ; \;\;\; \alpha = \alpha_* \frac{\sqrt{g}}{(s-1)} \tag{5.2}$$

$$q_s = \beta y \frac{dy}{dx} \;\; ; \;\;\; \beta = \beta_* \frac{g}{(s-1)w_f} \tag{5.3}$$

where, α_* and $\beta_* =$ dimensionless parameters related to bed load and suspended load, respectively; $g =$ gravitational acceleration; s and $w_f =$ specific gravity and fall velocity of the sand with $s = 2.6$ and $w_f = 2.0$ cm/s in this experiment. The dimensional parameters α and β depend on the sand characteristics even if α_* and β_* are constant. Equations (5.2) and (5.3) are valid only in the inner surf zone because the magnitudes of q_b and q_s increase seaward with the increase of the depth $h = y^{2/3}$. The original formulas of q_b and q_s without the approximations predict the seaward decrease of the magnitudes of q_b and q_s outside the surf zone (Kobayashi and Jung 2012).

The effect of q_n on the equilibrium profile based on Equation (5.1) can be assessed qualitatively using Equation (5.2) for the onshore rate q_b depending on h only and Equation (5.3) for the offshore rate q_s depending on h and (dh/dx), which is negative for h decreasing with the onshore coordinate x. The equilibrium profile with $q_n = 0$ should become gentler (steeper) when q_n becomes positive (negative) in order to decrease (increase) the offshore rate q_s at the given depth h. The gentler (steeper) profile implies the landward (seaward) shift of the shoreline as observed in the P (N) test in Figure 4.5.

Equations (5.1) – (5.3) are solved analytically

$$y - y_r + \frac{q_n}{\alpha} \ln\left|\frac{\alpha y - q_n}{\alpha y_r - q_n}\right| = \frac{\alpha}{\beta}(x_r - x) \; ; \; y_r = h_r^{1.5} \tag{5.4}$$

where, x_r and h_r = reference cross-shore location and depth on the equilibrium profile. For analytical convenience, Equation (5.4) is regarded to express x as a function of $y = h^{1.5}$. The equilibrium profile $x_e(y)$ for $q_n = 0$ is expressed as

$$y - y_r = \frac{\alpha}{\beta}(x_r - x_e) \; ; \; q_n = 0 \tag{5.5}$$

The reference location is normally taken as the shoreline ($h=0$) located at $x=x_o$. Equation (5.5) with $y_r = 0$ and $x_r = x_o$ yields

$$h = A(x_o - x_e)^{\frac{2}{3}} \; ; \; A = \left(\frac{\alpha}{\beta}\right)^{2/3} \quad \text{for} \quad q_n = 0 \tag{5.6}$$

which expresses the water depth h as a function of $(x_o - x_e)$, offshore distance from the shoreline. The dimensional parameter A in Equation (5.6) was estimated using laboratory and field data (Dean 1991). The expressions of α and β in Equations (5.2) and (5.3) indicate that the parameter A is proportional to $(w_f^2/g)^{1/3}$ as proposed by Kriebel et al. (1991). In the following, α and A are treated as independent parameters and ($\beta = \alpha / A^{1.5}$) because A is better known than β.

5.3   Horizontal Profile Shift

The horizontal shift $S(y)$ of the equilibrium profile $x(y)$ for arbitrary q_n from that for $q_n = 0$ is expressed as $S(y) = x(y) - x_e(y)$. Subtraction of Equation (5.5) from Equation (5.4) yields

$$S(y) = \frac{q_n}{\alpha A^{1.5}} F(y) \; ; \; F(y) = \ln \left| \frac{\alpha y_r - q_n}{\alpha y - q_n} \right| \tag{5.7}$$

where, $F(y) = 0$ at $y = y_r$ with $y_r = h_r^{1.5}$. The reference depth h_r is taken as the closure depth d_c in order to predict the shift $S(y)$ in the vicinity of the shoreline. The dimensionless function F is given by

$$F(y_*) = \ln \left| \frac{1 - q_*}{y_* - q_*} \right| \; ; \; y_* = (\frac{h}{d_c})^{1.5} \; ; \; q_* = \frac{q_n}{\alpha d_c^{1.5}} \tag{5.8}$$

which, is limited to the range of $0 \le h \le d_c$ and $0 \le y_* \le 1$. The normalized rate q_* is the ratio between the net rate q_n and the bed load transport rate q_b in Equation (5.2) at the closure depth d_c. For the N and P tests, the magnitude of q_* is found to be of the order of 0.002. The net rates q_n for the N and P tests are much smaller than the onshore and offshore sand transport rates. $|y_* - q_*| = q_*$ is used if $y < 2q^*$ for the case of $q_* > 0$ to avoid zero when $y_* = q_n$.

5.4 Comparison of the Analytical Model with Three Tests

The equilibrium profile model is compared with the Z, N, and P tests. The equilibrium profile of Z10 with $q_n = 0$ is compared with Equation (5.6) to estimate the parameter A. The shoreline location was at $x_o = 17.9$ m. The closure depth was $d_c = 0.2$ m at $x_c = 11.7$ m. Equation (5.6) with $h = 0.2$ m at $x_e = 11.7$ m yields $A = 0.059$ m$^{1/3}$. Figure 5.4 compares the measured and fitted profiles for Z10. The agreement is reasonable except for the step zone at the toe of the foreshore. The measured profiles of N20 and P20 could be fitted to Equation (5.6) with slightly different values of A but $A = 0.059$ m$^{1/3}$ is used for the N and P tests because A is supposed to depend on the sand characteristics only.

Measured and Analytical Profiles of Z10
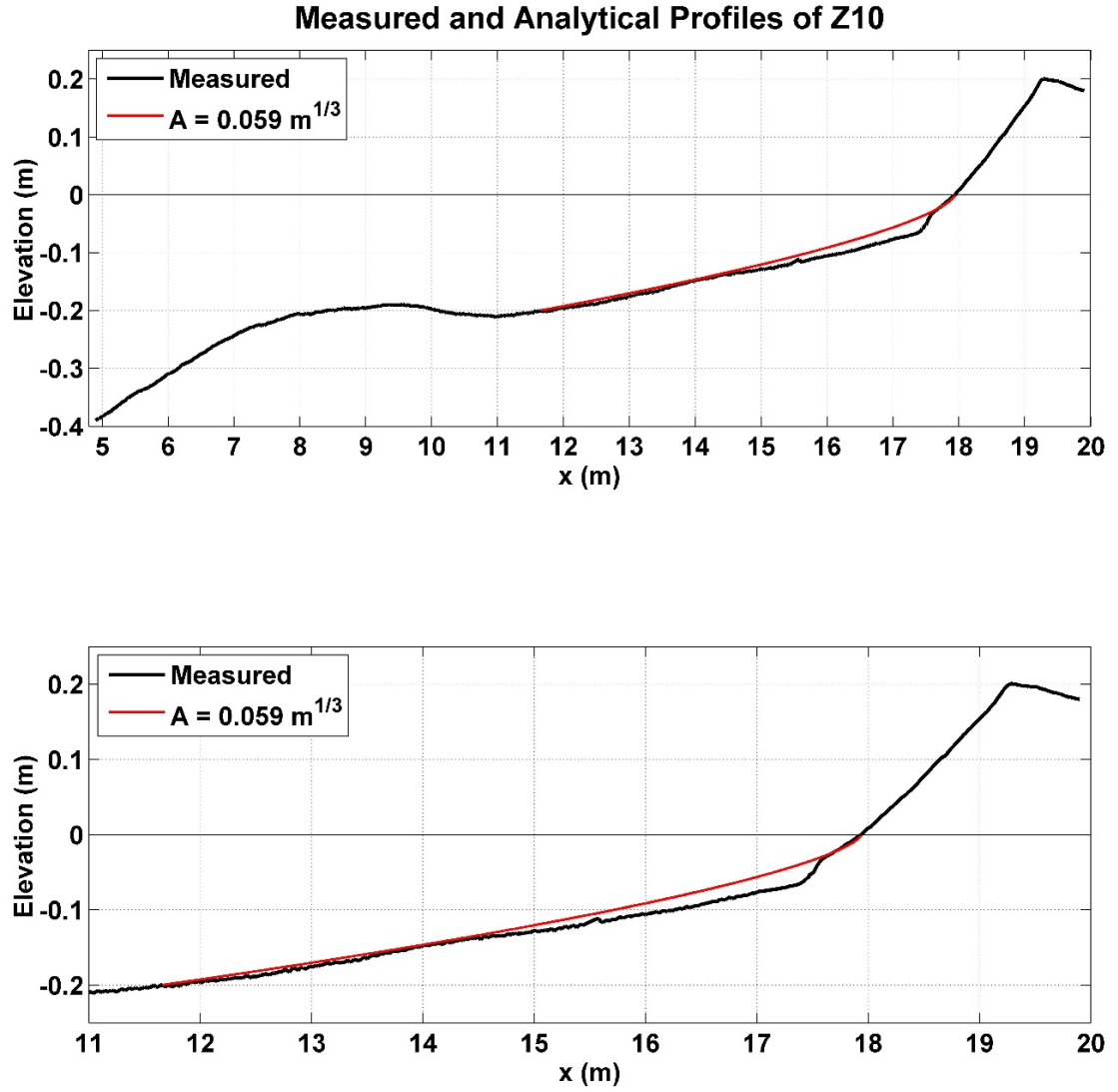
Figure 5.1:   Measured profile and analytical profiles for Test Z with fitted A=0.059 m$^{1/3}$ from x_c=11.7 m where x_0=17.9 m at zero elevation

The measured horizontal shift from the initial profile of N0 (same as Z10) to the final profile of N20 is compared with $S(y)$ given by Equation (5.7) with $y = h^{1.5}$. For the N test, q_n = -0.006 cm^2/s and d_c = 0.2 m. Figure 5.2 compares the measured and computed values of S at the given elevation $z = (-h)$. The dimensional parameter

α is calibrated to yield the measured shift S = -9 cm at the shoreline (z = 0). The calibrated value is $\alpha = 0.003$ m$^{1/2}$/s. The dimensionless parameters in Equations (5.2) and (5.8) are $\alpha_* = 0.0015$ and $q_* = 0.0022$. The computed shift S is limited to the zone of $z < 0$ below the SWL and decreases downward with $S = 0$ at the closure depth elevation $z = -0.2$ m. The measured horizontal shift of the order of 0.1 m on the gentle slope seaward of the step is not predicted by Equation (5.7) because the analytical model cannot predict the formation and migration of the step at the toe of the foreshore. Figure 5.6 compares the measured and computed profiles of N20. The computed profile is obtained by adding the computed horizontal shift in Figure 5.2 horizontally to the measured initial profile of N0 because the equilibrium profile of Equation (5.6) does not include the step-like feature of N0 (Z10) as shown in Figure 5.1. The agreement has improved because of the use of the measured equilibrium profile of Z10 for $q_n = 0$.

For the P test, the initial profile of P0 was not an equilibrium profile with $q_n = 0$ after the 4-cm increase of the SWL, which resulted in wave overtopping and overwash of the foreshore crest. Figure 5.4 compares the measured and computed horizontal profile shift from P0 and P20. Use is made in Equations (5.7) and (5.8) of $q_n = 0.0034$ cm^2/s (average during 8,000 s in Figure 3.5), $A = 0.059$ m$^{1/3}$ (same), calibrated $\alpha = 0.0015$ m$^{1/2}$/s (halved), and $d_c = 0.24$ m (4-cm SWL increase). The dimensionless parameters are $\alpha_* = 0.0008$ and $q_* = 0.0019$. The landward 8-cm shift of the shoreline at $z = 0$ did not represent the entire foreshore slope unlike in Figure 5.2 because of sand deposition on the upper foreshore. The measured horizontal shift below the foreshore included the profile adjustment after the 4-cm SWL increase and cannot be predicted by Equation (5.7). Figure 5.5 compares the

measured and computed profiles of P20. The computed profile is the sum of the initial profile of P0 and the computed shift S in Figure 5.4. The agreement of P20 is worse than that of N20 in Figure 5.3 partly because wave overwash was produced by the 4-cm SWL increase which created a non-equilibrium initial profile.
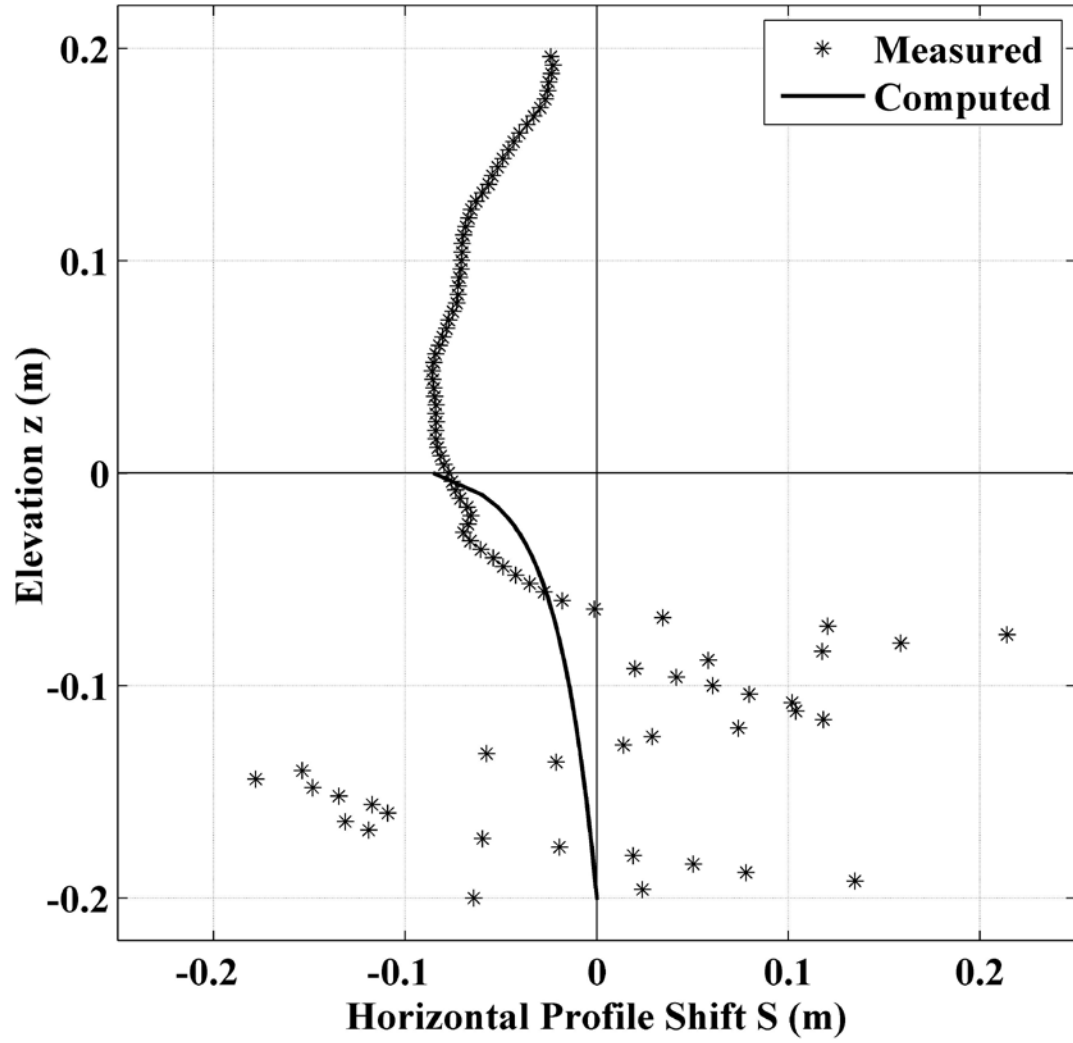
Figure 5.2:   Measured and computed horizontal profile shift from N0 to N20
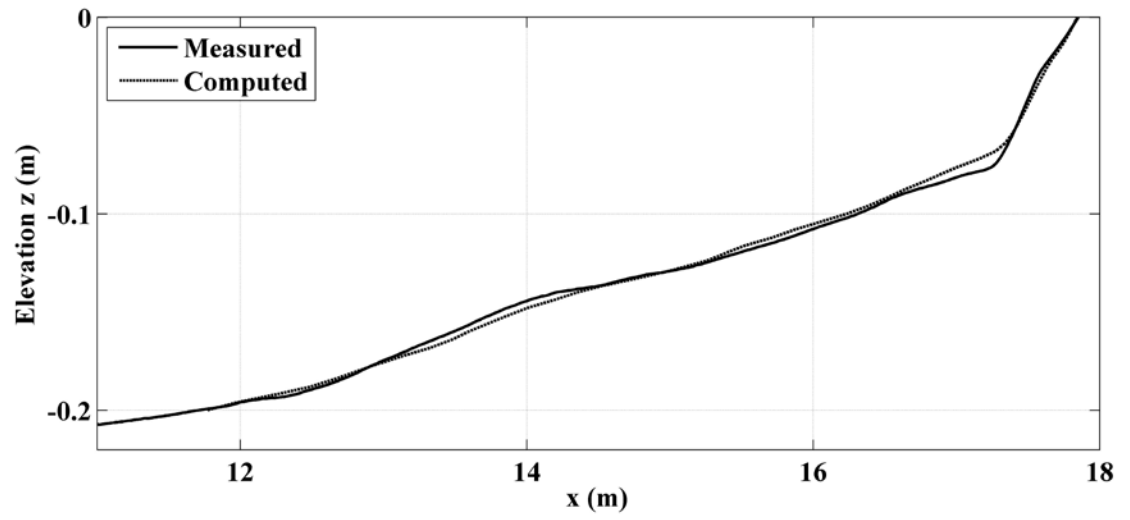
Figure 5.3: Measured and computed profile of N20 starting from initial profile of N0
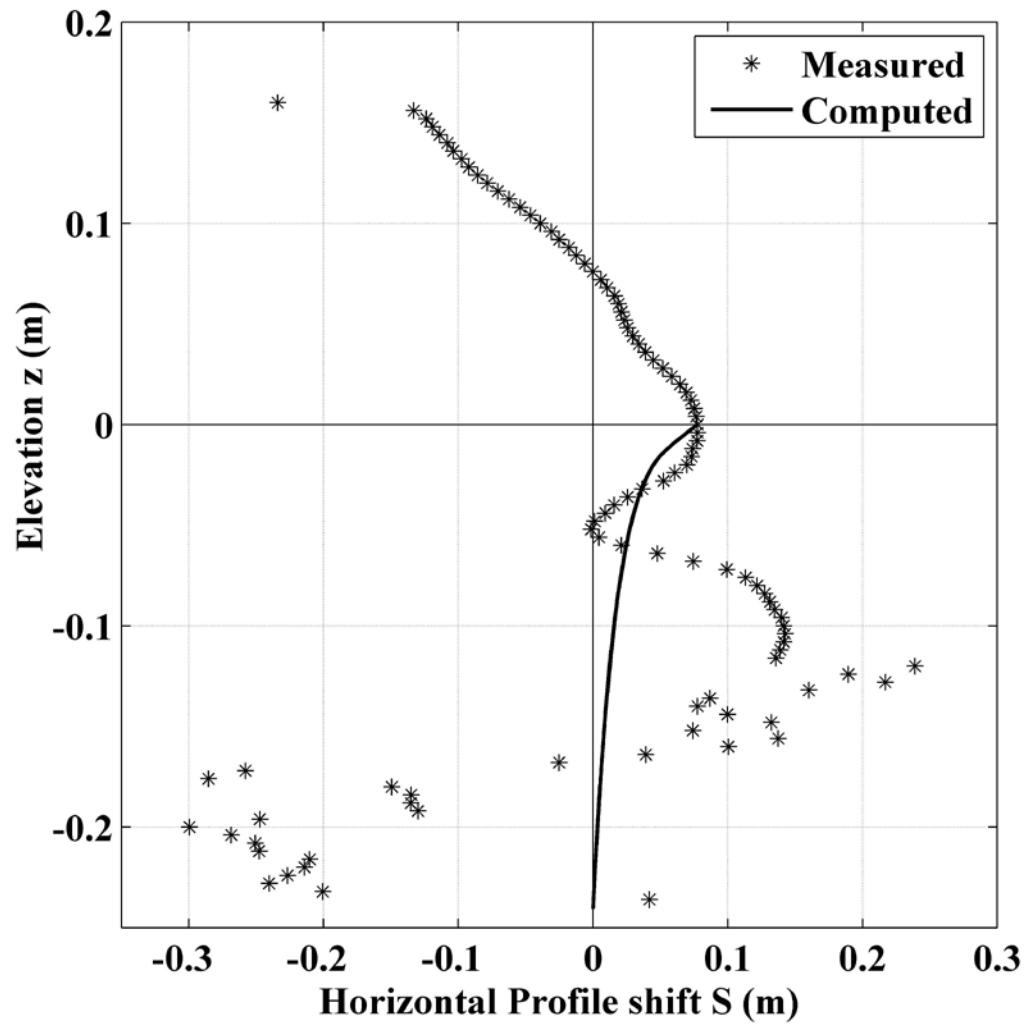
Figure 5.4:   Measured and computed horizontal shift from P0 to P20
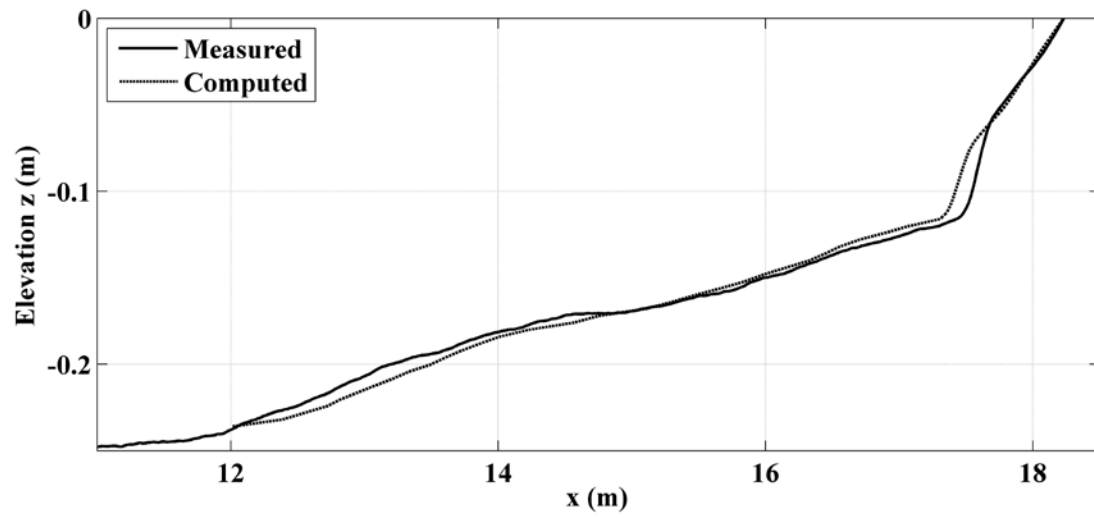
Figure 5.5: Measured and computed profile of P20 starting from initial profile of P0

Chapter 6

FIELD APPLICATION OF THE NEW MODEL

The simple equilibrium profile model with net cross-shore sand transport rate q_n may not be very accurate but may be used to estimate the shoreline shift of an equilibrium profile with $q_n = 0$ caused by periodic sand placement $q_n < 0$ near the shoreline or frequent sand overwash $(q_n > 0)$ resulting from sea level rise. The following application of Equations (5.7) and (5.8) evaluates the present beachfill design which does not account for the equilibrium profile modification caused by periodic beachfill placement.

The seaward shoreline displacement D caused by $q_n < 0$ is estimated as $D = [- S (y = 0)]$ in Equation (5.7).

$$D = \frac{-q_n}{\alpha A^{1.5}} \ln \left| \frac{1-q_*}{-q_*} \right| \; ; \; q_* = \frac{q_n}{\alpha d_c^{1.5}} \tag{6.1}$$

The value of $A = 0.059$ m$^{1/3}$ is kept the same because the functional relation between D and A is simple. For the N test, $\alpha = 0.003$ m$^{1/2}$/s, $(-q_n) = 0.006$ cm^2/s (19 m^2/y), and $d_c = 0.2$ m.
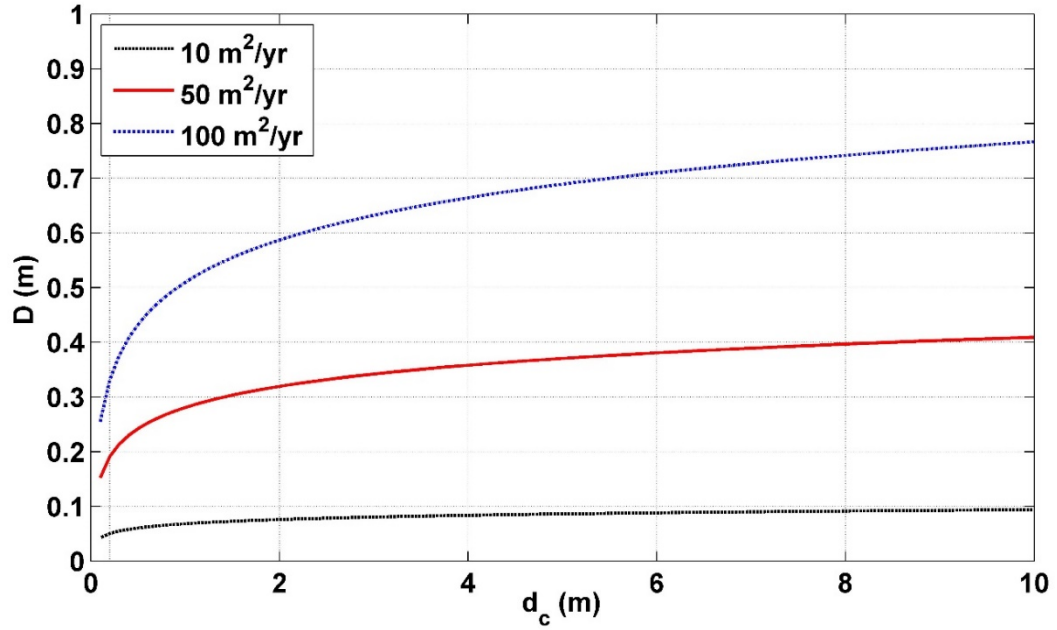
Figure 6.1: Seaward shoreline displacement D (m) as a function of closure depth d_c (m) for $\alpha = 0.003$ m$^{1/2}$/s and $(-q_n)$= 10 m^2/yr, 50 m^2/yr, and 100 m^2/yr

Figure 6.1 shows the seaward shoreline displacement D as a function of the closure depth d_c for $(-q_n)$ = 10, 50, and 100 m^2/y. The increase of D with the increase of d_c is rapid at d_c =0.1 m but becomes slow for d_c exceeding 2 m. For field applications with d_c of about 6 m, D is not very sensitive to d_c. It is noted that the present model allows net cross-shore sand transport at the closure depth. The displacement D increases with the rate of beachfill placement which is normally less than 100 m^2/y. Figure 6.1 suggests that the displacement D should be less than 1 m. The dimensional parameter α is supposed to be constant for the sand with $s = 2.6$ in light of Equation (5.2) but $\alpha = 0.0015$ m$^{1/2}$/s was necessary to reproduce the measured shoreline shift of P20. Figure 6.2 shows the displacement D as a function of d_c for $(-q_n)$ = 50 m^2/y and α = 0.001, 0.002, and 0.003 m$^{1/2}$/s.

The displacement D is sensitive to α but may not exceed 1 m. Equation (6.1) will need to be verified using large-scale laboratory data and field data.
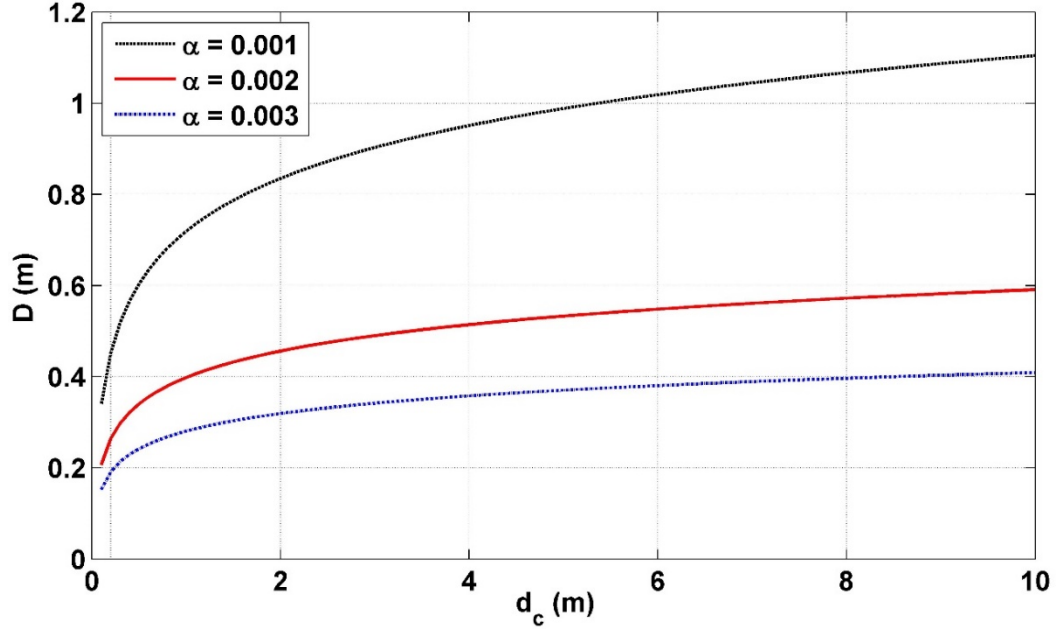
Figure 6.2:   Seaward shoreline displacement D (m) as a function of closure depth d_c (m) for $(-q_n) = 50$ m^2 and $\alpha = 1{\times}10^{-3}$, $2{\times}10^{-3}$ and $3{\times}10^{-3}$ m$^{1/2}$/s

Chapter 7

COMPARISION WITH NUMERICAL PROFILE EVOLUTION MODEL

This chapter explains the cross-shore numerical model CSHORE and compares CSHORE with the three tests. The numerical model of CSHORE is described in detail in Kobayashi (2016).

7.1   Cross-Shore Model (CSHORE)

The components of CSHORE for normally incident waves used in this study include: a combined wave and current model based on time-averaged continuity, momentum, wave action, and roller energy equations; a sediment transport model for bed load and suspended load coupled with the continuity equation of bottom sediment; and a probabilistic swash model on an impermeable bottom. The fine sand used in the experiment is assumed to be impermeable. Input to the numerical model for each test includes the measured bottom elevation z_b of sand surface at time t = 0, measured values of $\overline{\eta}$, H_{mo}, and T_p at x = 0 for all the runs in the tests. The input parameters for CSHORE are taken as standard values in order to assess the degree of agreement in light of previous comparisons discussed in Kobayashi (2016).

The cross-shore model CSHORE computes the mean and standard deviation (SD) of the free surface elevation above SWL and the depth-averaged cross-shore velocity U above the bottom elevation z_b. The cross-shore bed load and suspended load transport rates q_b and q_s are estimated using the empirical formulas in CSHORE.

7.2 Cross-Shore Wave Transformation

The CSHORE is compared with the measured data of the cross-shore wave transformation, wave overtopping and sand overwash rates, and beach profile evolutions for Z, N and P tests. The measured cross-shore variations of $\bar{\eta}$, σ_η, Pw, $\bar{U}$, and σ_U are plotted for 10 or 20 runs with constant SWL in each test together with the computed cross-shore variations in Figures 7.1-7.3. These hydrodynamic variables are predicted within errors of about 20% except for WG8 at x = 18.6 m in the swash zone.
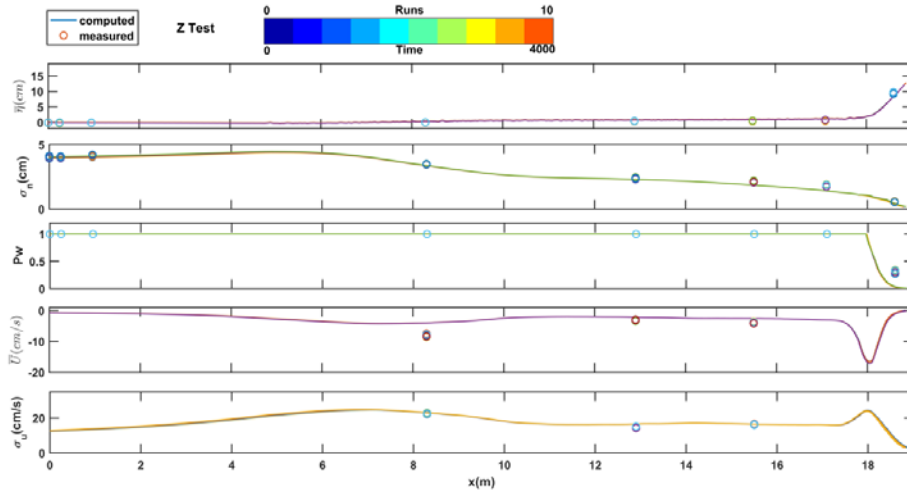
Figure 7.1: Mean and standard deviation of free surface elevation $\bar{\eta}$ and horizontal velocity $\bar{U}$ together with wet probability P_w for 10 runs during time t = 0 to 4,000 s for Test Z

38
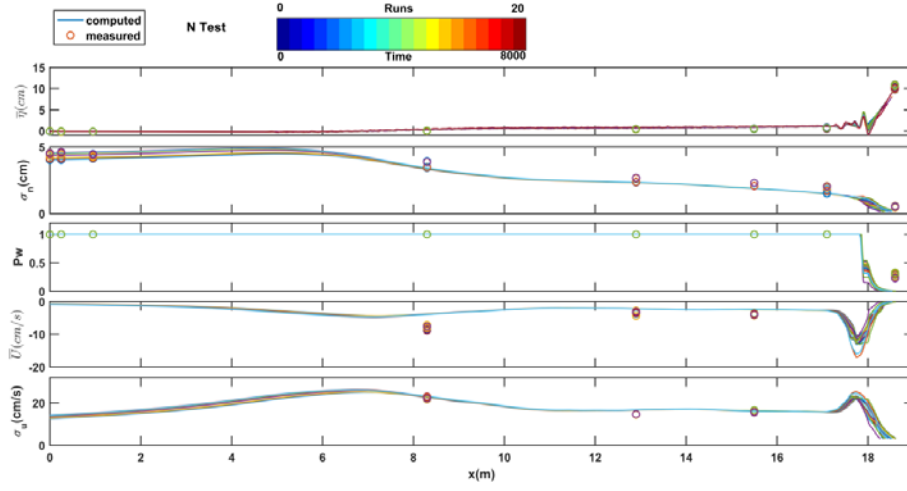
Figure 7.2: Mean and standard deviation of free surface elevation $\bar{\eta}$ and horizontal velocity $\bar{U}$ together with wet probability P_w for 20 runs during time t = 0 to 8,000 s for Test N
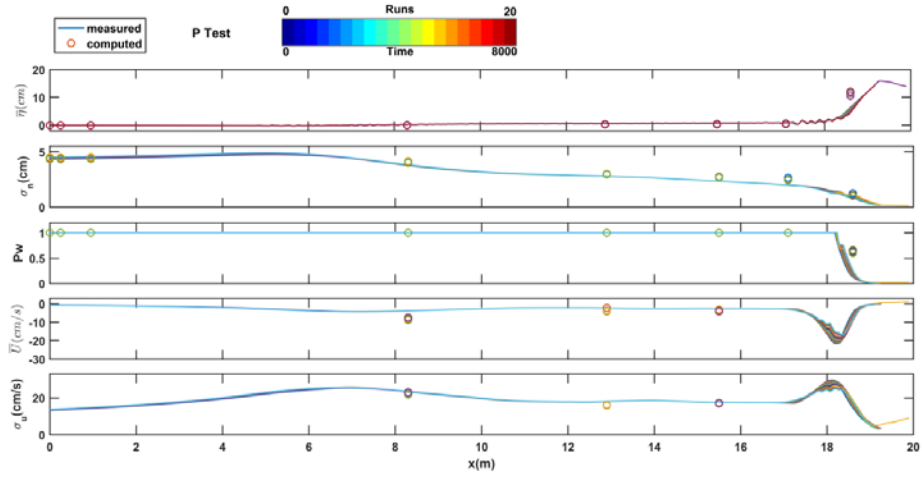
Figure 7.3: Mean and standard deviation of free surface elevation $\bar{\eta}$ and horizontal velocity $\bar{U}$ together with wet probability P_w for 20 runs during time t = 0 to 8,000 s for Test P

7.3 Wave Overtopping and Overwash Rates

The average wave overtopping rate q_o and sand overwash rate q_{bs} during each run for Test P are shown in Figure 7.4. These small rates are associated with the mean water depth on the berm of the order of 0.1 cm. No overtopping and overwash occurred in the Z and N during t = 0 – 4,000 s and t = 0 – 8,000 s respectively. The small rates are difficult to predict accurately.
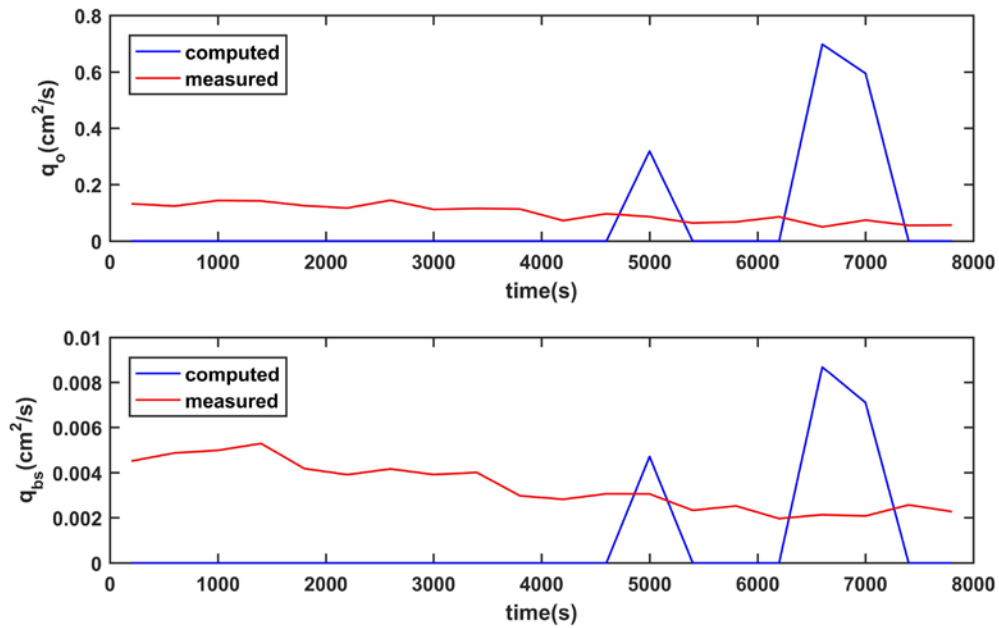
Figure 7.4:   Water overtopping rate q_o and sand overwash rate q_{bs} during Test P

7.4 Beach Profile Evolution

The initial, measured and computed profiles for the Z, N and P tests are compared in Figures 7.5 ,7.6 and 7.7, respectively, where the initial profile at t = 0 is plotted to indicate the degree of the profile change at the given time. The profiles are plotted at t = 2000 s and t = 4000 s for the Z test. For the N and P tests, the profiles are

plotted at t = 2000 s , t = 4,000 s and t = 8,000 s. The profile changes are less than 2mm for x < 11m and hence these figures are limited to x > 11 m. CSHORE cannot consistently predict small accretional and erosional profile changes of quasi-equilibrium profiles caused by periodic sand placement and overwash.
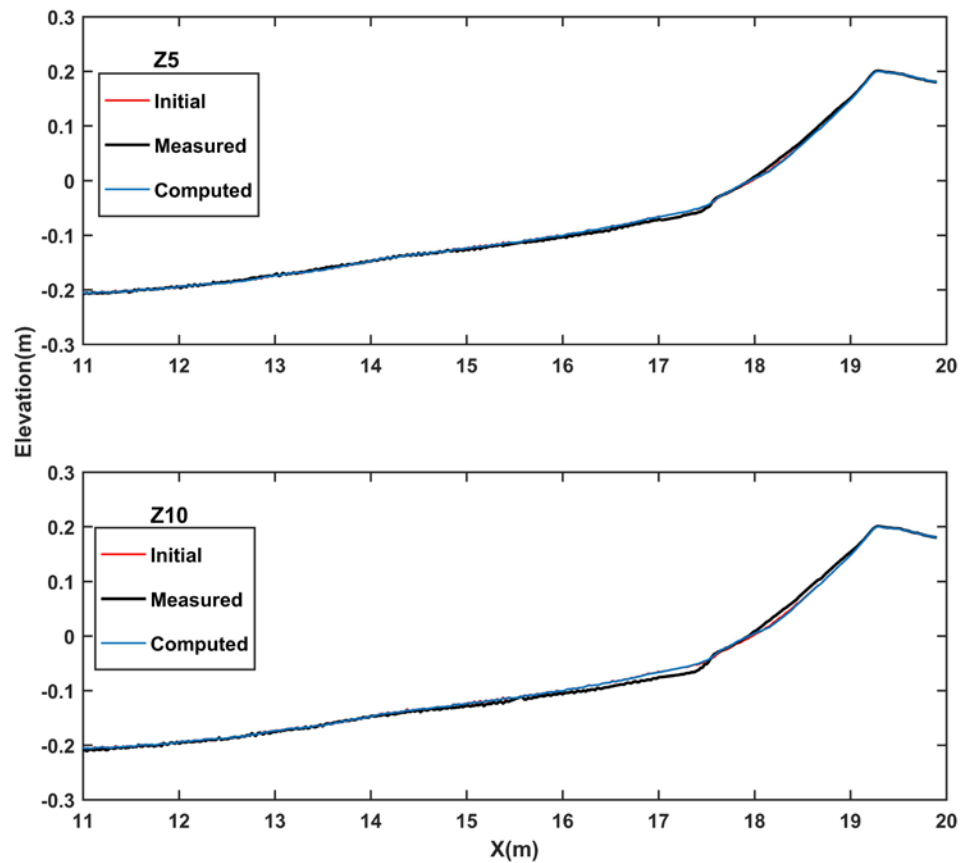
Figure 7.5: Initial, measured and computed profiles for t= 2,000 s and t= 4,000 s of Test Z
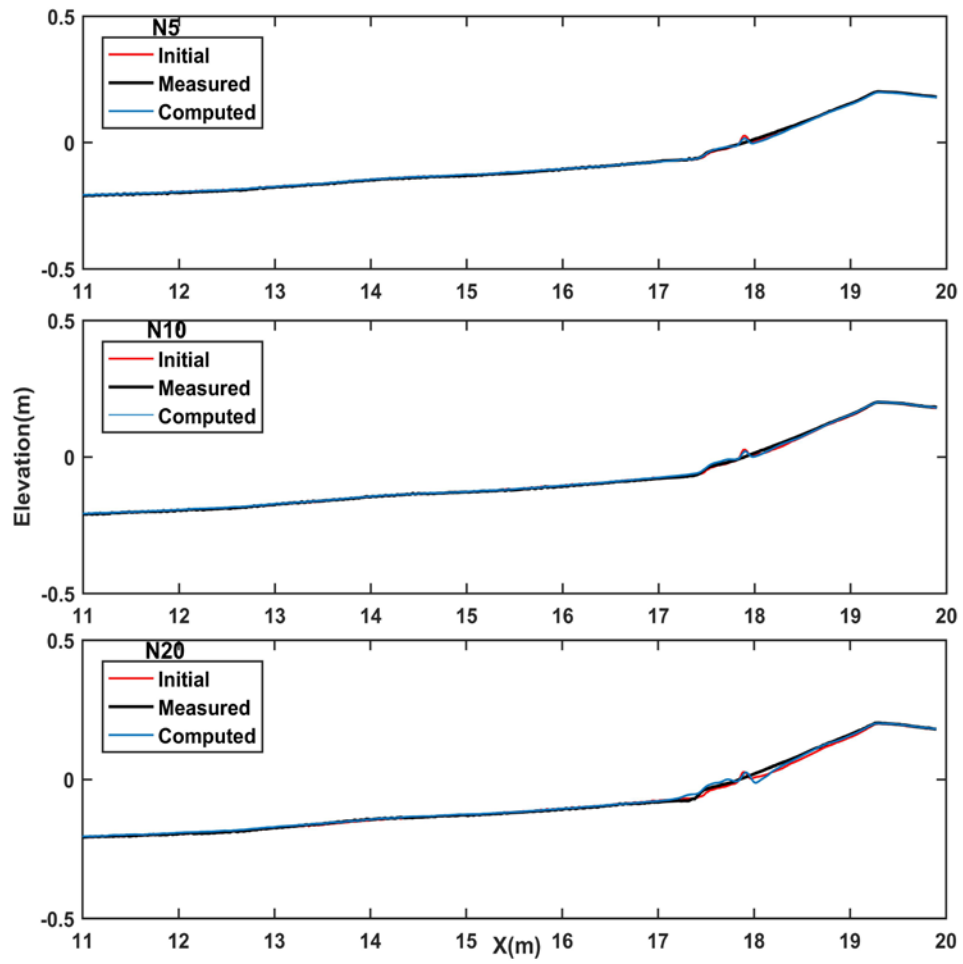
Figure 7.6:   Initial, measured and computed profiles at t= 2,000 s , t= 4,000 s and
               t = 8,000 s for Test N
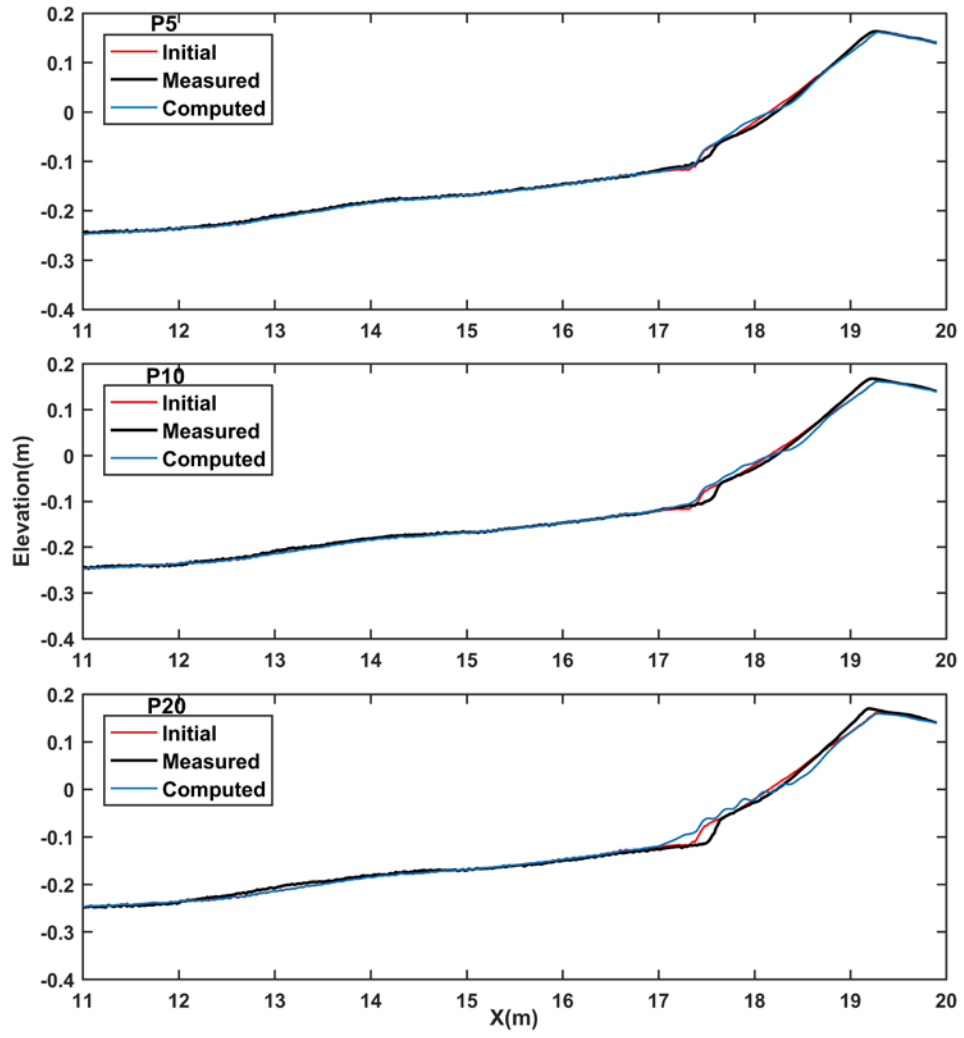
Figure 7.7: Initial, measured and computed profiles at t= 2,000 s , t= 4,000 s and t = 8,000 s for Test P

Chapter 8

CONCLUSIONS

8.1   Experimental Findings

Three tests consisting of fifty 400-s runs were conducted in a small-scale experiment to quantify the differences among quasi-equilibrium profiles in the inner surf zone on a sand beach under the conditions of zero, negative (offshore), and positive (onshore) net cross-shore sand transport. A step-like feature formed at the toe of the foreshore and migrated in the three tests.   The negative net sand transport resulting from periodic sand placement near the shoreline translated the foreshore slope seaward and made the beach profile steeper.   The positive net sand transport caused by wave overtopping and overwash, shifted the shoreline landward and made the inner surf zone profile gentler. However, the profile changes among the three tests were relatively small and the shoreline shifts were less than 0.1 m. The conventional model based on the conservation of sand volume and the cross-shore translation of an entire active profile underpredicts the shoreline changes measured in this experiment because only a portion of the profile translated.

8.2   Analytical Modeling

An analytical model for an equilibrium profile with net cross-shore sand transport is developed by approximating the bed load and suspended load formulas by Kobayashi et al. (2008) in the inner surf zone. The analytical model produces the equilibrium profile equation by Dean (1991) for the case of zero net cross-shore sand transport. The model predicts the seaward (landward) shift of the equilibrium profile caused by negative (positive) net cross-shore sand transport.   The model cannot

predict the migration of the step. The predicted horizontal shift is the maximum at the shoreline and approaches zero at the closure depth. Two parameters in the model are calibrated using the three tests. The equilibrium profile parameter A is calibrated using the equilibrium profile with net sand transport rate $q_n = 0$. The bed load parameter α calibrated for the two tests with $q_n < 0$ and $q_n > 0$ differs by a factor of two. The calibrated model is used to estimate the seaward shift of the shoreline on periodically-nourished beaches of prototype scale. The estimated shift is of the order of 1 m or less but will need to be verified using large-scale laboratory data.

The analytical model will need to be extended to oblique waves and verified using field data. Oblique waves and longshore current modify the net cross-shore sand transport rate [e.g., Kobayashi et al. (2009)] which is assumed constant in the inner surf zone. Long-term onshore sand transport from outside the inner surf zone (Dean and Houston 2016) may affect the inner surf zone profile. Extreme storms may cause significant offshore suspended sand transport beyond the closure depth [e.g., Madsen et al. (1994)]. Net cross-shore sand transport outside the closure depth is uncertain at present. The findings of this study may encourage careful analyses of nourished and overwashed beach profile and shoreline data in the future because the predicted shift is relatively small.

8.3   Numerical Modeling

The accuracy of cross-shore numerical model CSHORE is assessed using the three tests. The mean and standard deviation of free surface elevation and velocity are predicted within errors of about 20% as in previous comparisons. However, CSHORE cannot consistently predict small erosional and accretional profile changes of quasi-equilibrium profiles caused by periodic sand placement and overwash. It is

challenging to develop a reliable model that can predict long-term beach profile evolution including periodic beachfill placement or frequent overwash.

REFERENCES

Dean, R.G. (1991). "Equilibrium beach profiles: Characteristics and applications." J. Coastal Res., 7(1), 53-84.

Dean, R.G., and Houston, J.R. (2016). "Determining shoreline response to sea level rise." Coastal Eng., 114, 1-8.

Figlus, J., Kobayashi, N., Gralher, C., and Iranzo, V. (2011). "Wave overtopping and overwash of dunes." J. Waterway, Port, Coastal, Ocean Eng., 10.1061/(ASCE)WW.1943-5460.0000060, 26-33.

Houston, J.R. (2016). "Beach nourishment as an adaptation strategy for sea level rise: A Florida east coast perspective." Shore & Beach, 84(2), 3-12.

Jiménez, J.A., Sallenger, A.H., and Fauver, L. (2006). "Sediment transport and barrier island changes during massive overwash events." Proc. 30th Coastal Engineering Conf., World Scientific, Singapore, 2870-2879.

Kobayashi, N. (2016). "Coastal sediment transport modeling for engineering applications." J. Waterway, Port, Coastal, Ocean Eng., 10.1061/(ASCE)WW. 1943-5460.0000347.

Kobayashi, N., Buck, M., Payo, A., and Johnson, B. (2009). "Berm and dune erosion during a storm." J. Waterway, Port, Coastal, Ocean Eng., 10.1061/(ASCE)0733-950X(2009)135:1(1), 1-10.

Kobayashi, N., and Jung, H. (2012). "Beach erosion and recovery." J. Waterway, Port, Coastal, Ocean Eng., 10.1061/(ASCE)WW.1943-5460.0000147, 473-483.

Kobayashi, N., Payo, A., and Schmied, L. (2008). "Cross-shore suspended sand and bed load transport on beaches." J. Geophys. Res., 113(C7), C07001.

Kriebel, D.L., Kraus, N.C., and Larson, M. (1991). "Engineering methods for predicting beach profile response." Proc. Coastal Sediments 1991, ASCE, Reston, VA, 557-571.

Madsen, O.S., Chisholm, T.A., and Wright, L.D. (1994). "Suspended sediment transport in inner shelf waters during extreme storms." Proc. 24th Coastal Engineering Conf., World Scientific, Singapore, 1849-1864.

Rosati, J.D., and Stone, G.W. (2009). "Geomorphologic evolution of barrier islands along the northern U.S. Gulf of Mexico and implications for engineering design in barrier restoration." J. Coastal Res., 25(1), 8-22.

USACE (U.S. Army Corps of Engineers). (2003). Coastal engineering manual, Washington, D.C.

Appendix

CROSS-SHORE SEDIMENT TRANSPORT TESTS

A.1   Zero (Z) Net Cross-shore Sediment Transport Test
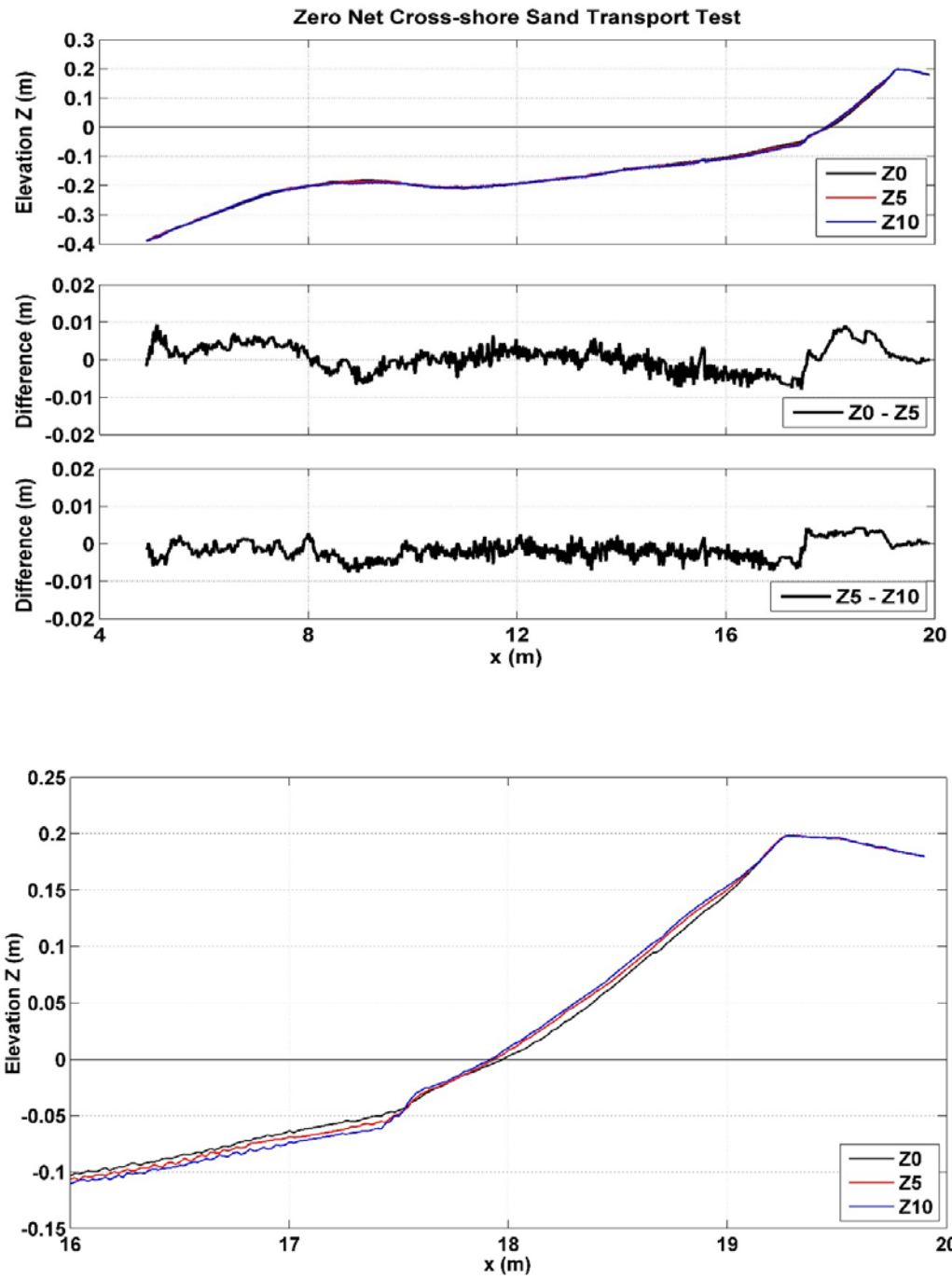
Figure A.1: Zero (Z) net cross-shore sediment transport test with 10 runs indicated by the numeral 1-10. For example, Z5 is run 5 in test Z. The measured profiles were Z0 before the Z test, Z5 after 5 runs, and Z10 after 10 runs. The elevation z is zero at the still water level in 88-cm water depth.

Table A.1: Incident wave characteristics for Test Z

Run	H_{mo} (cm)	H_{rms} (cm)	H_s (cm)	T_p (s)	T_s (s)	R
Z1	16.33	11.54	15.53	2.62	2.09	0.128
Z2	16.46	11.64	15.62	2.62	2.09	0.127
Z3	16.33	11.55	15.50	2.62	2.04	0.129
Z4	16.52	11.68	15.74	2.62	2.05	0.131
Z5	16.71	11.81	15.85	2.62	2.06	0.123
Z6	16.47	11.65	15.77	2.62	2.09	0.129
Z7	16.79	11.87	16.02	2.62	2.09	0.127
Z8	16.89	11.94	16.12	2.62	2.08	0.121
Z9	16.98	12.00	16.28	2.62	2.06	0.129
Z10	16.99	12.01	16.28	2.62	2.08	0.128
Average	**16.65**	**11.77**	**15.87**	**2.62**	**2.07**	**0.127**

Table A.2:　Mean free-surface elevation $\bar{\eta}$ (cm) at seven wave gauge locations

Run	WG1	WG2	WG3	WG4	WG5	WG6	WG7
Z1	-0.12	-0.11	-0.18	-0.10	0.29	0.41	0.55
Z2	-0.17	-0.16	-0.18	-0.07	0.34	0.41	0.56
Z3	-0.15	-0.27	-0.17	-0.06	0.35	0.40	0.54
Z4	-0.14	-0.12	-0.18	-0.06	0.35	0.41	0.55
Z5	-0.13	-0.17	-0.17	-0.06	0.37	0.42	0.58
Z6	-0.09	-0.19	-0.19	-0.07	0.27	0.32	0.42
Z7	-0.19	-0.26	-0.20	-0.04	0.36	0.46	0.73
Z8	-0.19	-0.33	-0.22	-0.06	0.38	0.46	0.73
Z9	-0.15	-0.12	-0.19	-0.04	0.38	0.42	0.57
Z10	-0.20	-0.14	-0.18	-0.02	0.36	0.44	0.54
Average	**-0.15**	**-0.19**	**-0.19**	**-0.06**	**0.35**	**0.42**	**0.58**

Table A.3:　Free-surface standard deviation σ_{η} (cm) at seven wave gauge locations

Run	WG1	WG2	WG3	WG4	WG5	WG6	WG7
Z1	3.93	3.94	4.05	3.46	2.29	2.05	1.70
Z2	3.97	3.98	4.07	3.47	2.31	2.07	1.72
Z3	3.93	3.95	4.04	3.44	2.31	2.07	1.72
Z4	3.99	4.00	4.07	3.46	2.32	2.07	1.72
Z5	4.04	4.05	4.13	3.46	2.31	2.06	1.73
Z6	3.99	3.97	4.12	3.50	2.45	2.20	1.90
Z7	4.06	4.04	4.17	3.48	2.37	2.09	1.86
Z8	4.10	4.08	4.18	3.49	2.39	2.10	1.87
Z9	4.11	4.08	4.21	3.49	2.39	2.10	1.86
Z10	4.12	4.10	4.20	3.51	2.37	2.10	1.87
Average	**4.02**	**4.02**	**4.12**	**3.48**	**2.35**	**2.09**	**1.80**

Table A.4: Wet probability P_w, its mean free-surface elevation $\bar{\eta}$ (cm) and free-surface standard deviation σ_η (cm) at WG8

Run	t (s)	P_w	Z_b (cm)	$\bar{h}$ (cm)	$\bar{\eta}$ (cm)	σ_η (cm)
	0		8.30			
Z1	200	0.31	8.35	1.39	9.74	0.59
Z2	600	0.30	8.46	0.71	9.17	0.60
Z3	1000	0.27	8.57	0.68	9.25	0.58
Z4	1400	0.33	8.68	0.58	9.26	0.57
Z5	1800	NA	8.79	NA	NA	NA
	2000		8.85			
Z6	2200	NA	8.89	NA	NA	NA
Z7	2600	0.31	8.99	0.58	9.57	0.53
Z8	3000	0.30	9.09	0.65	9.74	0.53
Z9	3400	0.34	9.18	0.62	9.80	0.53
Z10	3800	0.33	9.28	0.58	9.86	0.58
	4000		9.33			
Average		**0.31**		**0.72**	**9.47**	**0.56**

NA implies "not available" data

Table A.5: Mean cross-shore velocity $\overline{U}$ and standard deviation σ_U of the 2D ADV co-located with WG4 at $x = 8.30$ m, Red Vectrino co-located with WG5 at $x = 12.90$ m and Blue Vectrino co-located with WG6 at $x = 15.52$ m

Run	2D ADV at WG4		Red Vectrino at WG5		Blue Vectrino at WG6	
	$\overline{U}$ (*cm/s*)	σ_U (*cm/s*)	$\overline{U}$ (*cm/s*)	σ_U (*cm/s*)	$\overline{U}$ (*cm/s*)	σ_U (*cm/s*)
Z1	-8.57	22.73	-3.13	14.91	NA	NA
Z2	-8.24	22.55	-2.90	14.99	-3.79	16.27
Z3	-8.03	22.60	-2.94	15.02	-4.18	16.03
Z4	-8.16	22.37	-3.00	15.00	-3.87	16.34
Z5	-7.51	22.16	-2.97	14.96	-4.18	16.17
Z6	-8.59	22.48	-3.33	15.08	-3.58	16.55
Z7	-7.75	22.48	NA	NA	NA	NA
Z8	-8.41	22.82	-3.41	14.84	-3.88	16.34
Z9	-7.82	22.91	-3.12	14.89	-3.76	16.29
Z10	-8.36	22.61	-3.12	15.09	-4.21	16.29
Average	**-8.14**	**22.57**	**-3.10**	**14.98**	**-3.93**	**16.29**

NA implies "not available" data

A.2 Negative (N) Net Cross-shore Sediment Transport Test

Figure A.2: Negative (N) net cross-shore sediment transport test with 20 runs. The initial profile N0 corresponds to the profile Z10 added with the placed sand at the shoreline
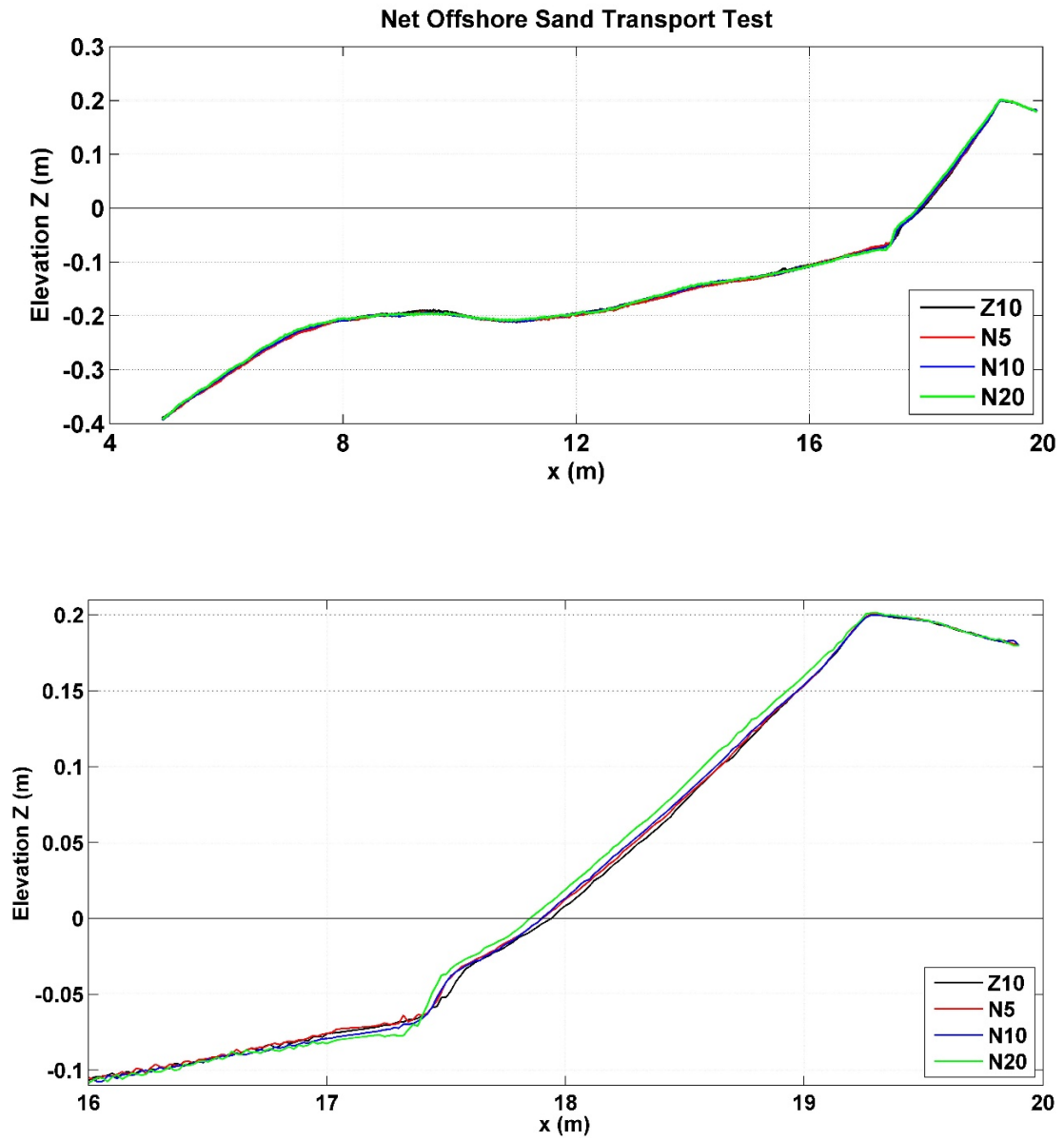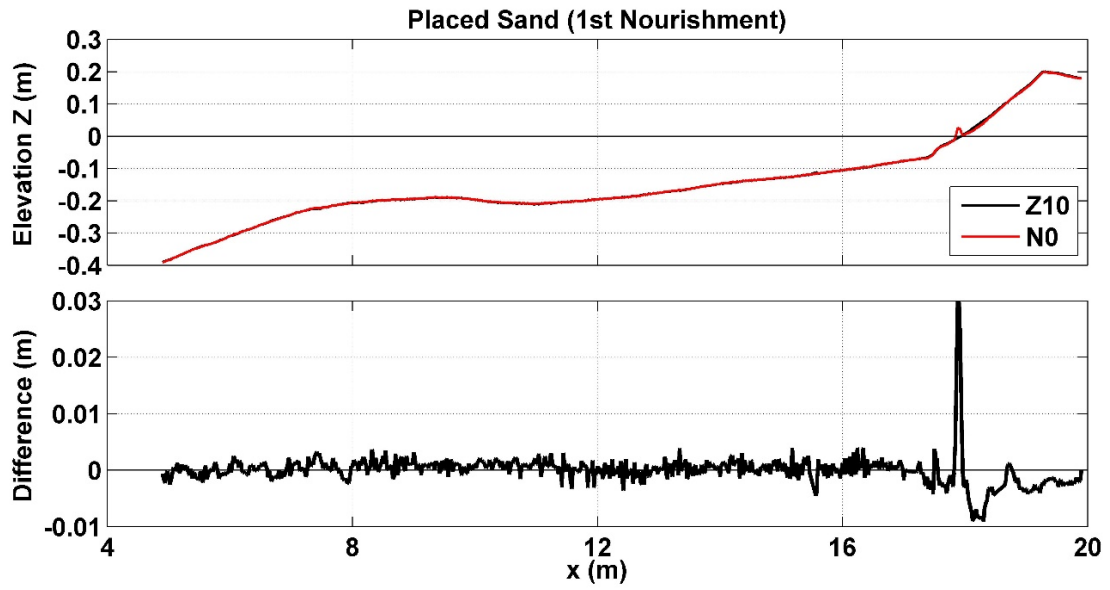
Figure A.3   Final profile for zero net cross-shore sand transport test (Z10) and initial profile for net offshore sand transport test (N0) with placed sand
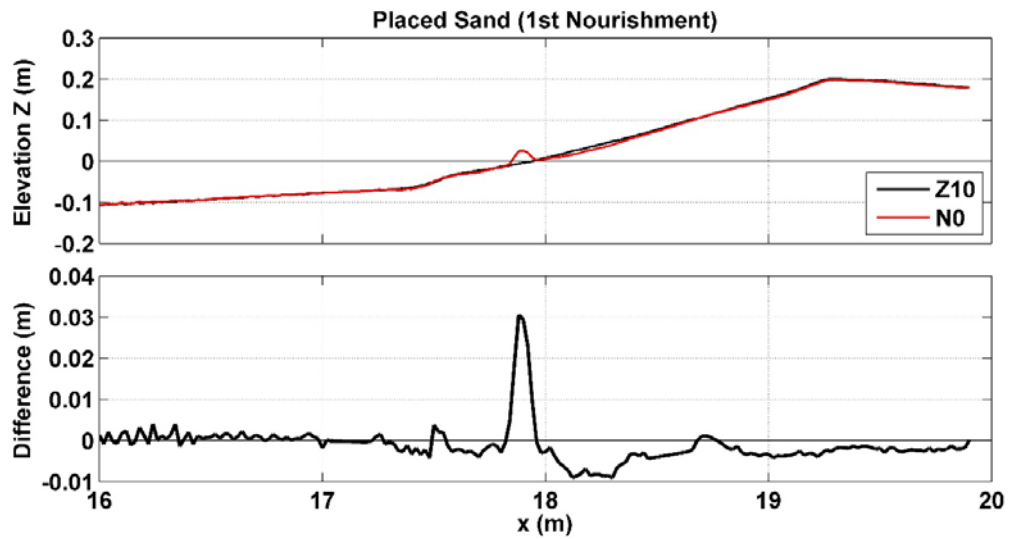
Figure A.4: Enlarged view of Figure A.3 near the shoreline

* Cross dune area (dune difference area above 0) = 22 cm^2
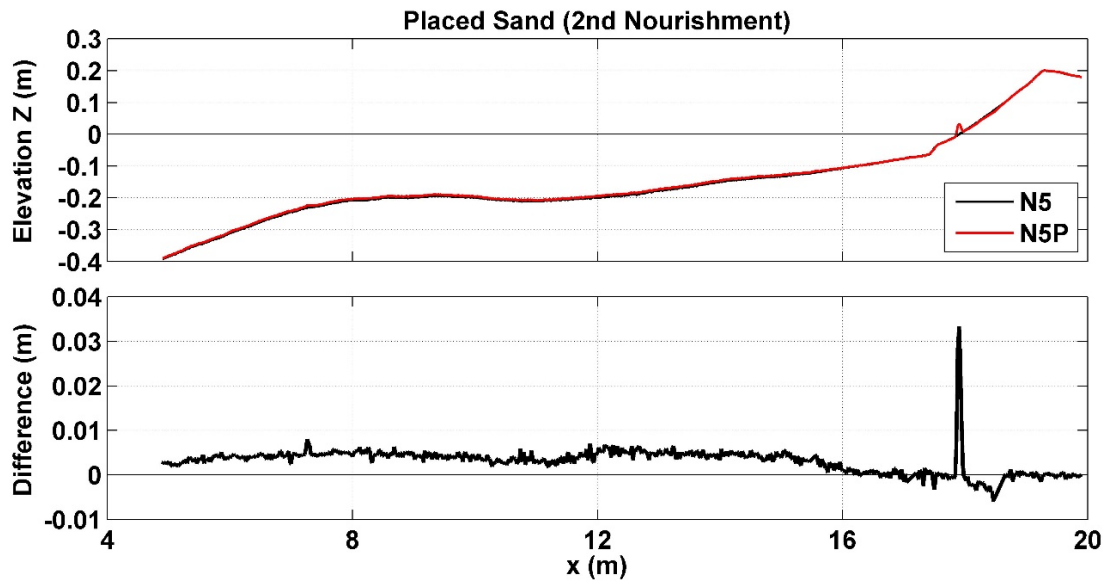
Figure A.5: Profile after 5 runs for net offshore sand transport test (N5) and profile
with placed sand for net offshore sand transport test (N5P)
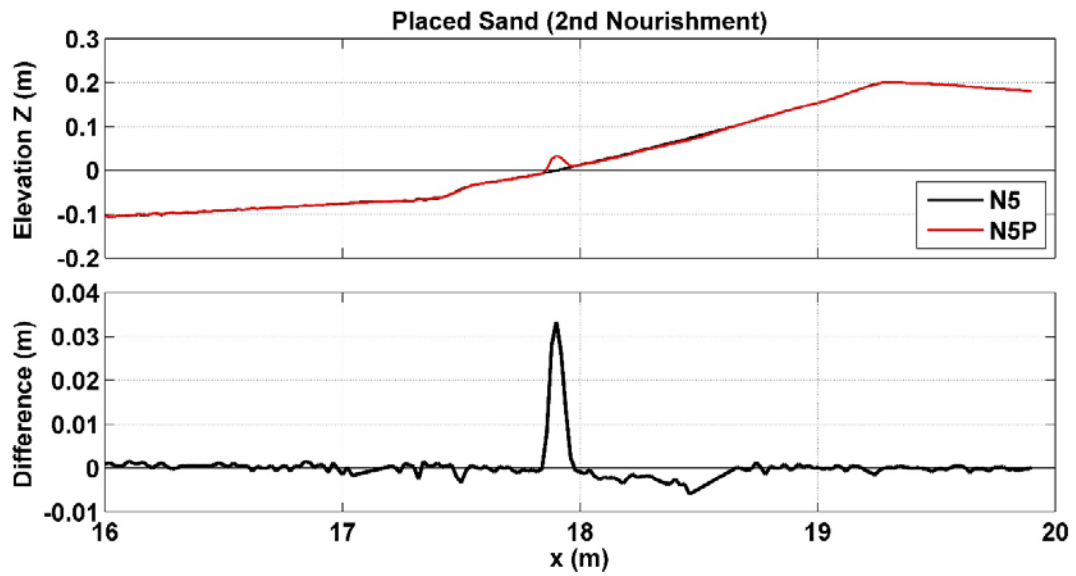
Figure A.6: Enlarged view of Figure A.5 near the shoreline

* Cross dune area (dune difference area above 0) = 22 cm^2
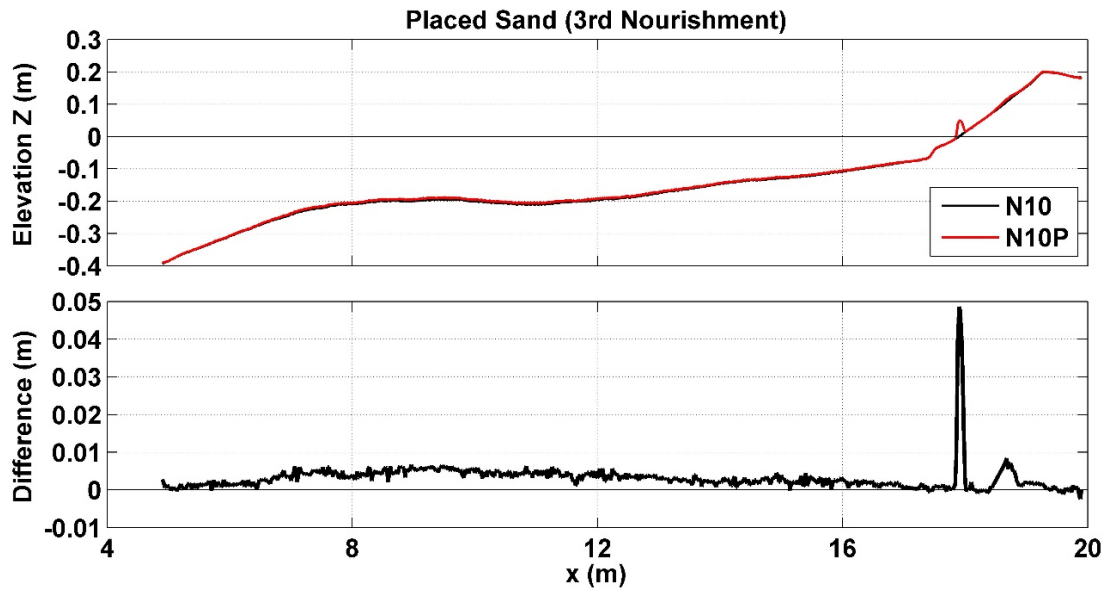
Figure A.7: Profile before sand placement (N10), and profile (N10P) with the placed sand after run N10 and before run N11
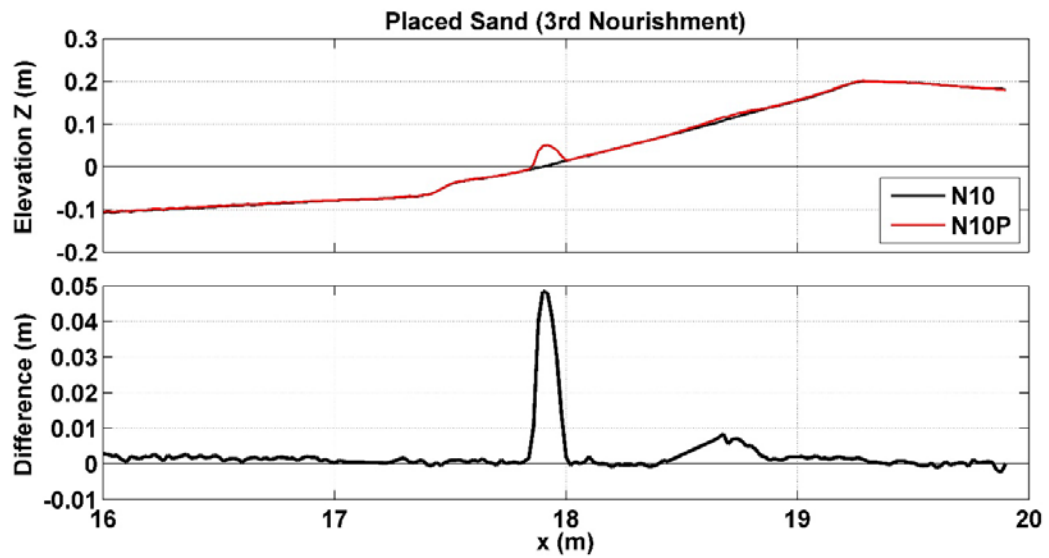
Figure A.8: Enlarged view of Figure A.7 near the shoreline

* Cross dune area (dune difference area above 0) = 45 cm^2
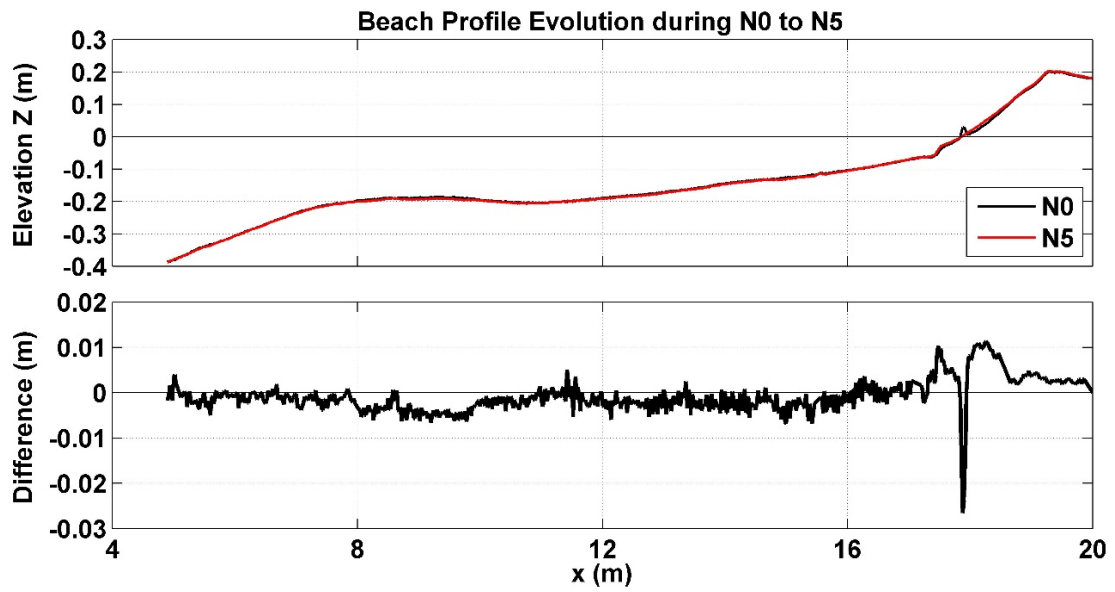
Figure A.9: Initial dune profile (N0) and profile after 5 runs (N5) for net offshore sand transport test. Sand was placed again after run N5 to produce the profile N5P with placed sand before run N6
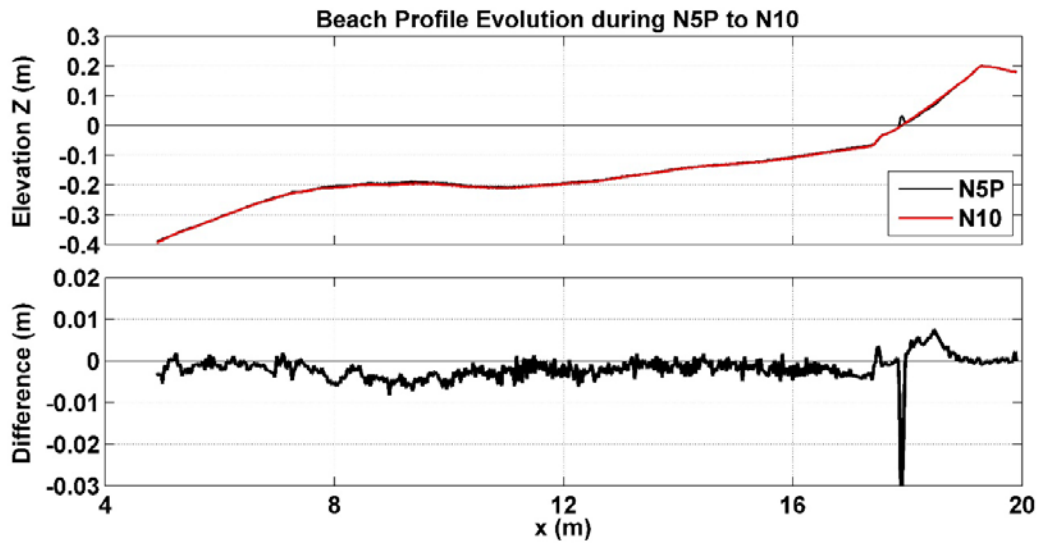
Figure A.10: Profile with placed sand and profile after 5 additional runs (N10) for net offshore sand transport test
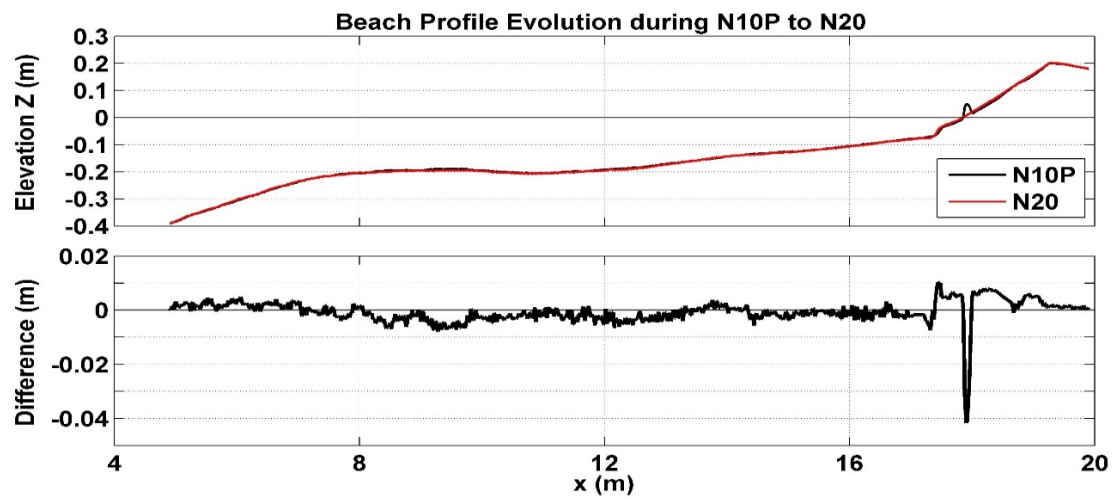
Figure A.11: Measured profiles N10P and N20 after additional 10 runs for net offshore
sediment transport test

Figure A.12: Placed sand near the shoreline for N test with no wave overtopping and overwash

Table A.6: Incident wave characteristics for Test N

Run	H_{mo} (cm)	H_{rms} (cm)	H_s (cm)	T_p (s)	T_s (s)	R
N1	16.79	11.87	16.11	2.62	2.06	0.129
N2	16.85	11.91	16.18	2.62	2.09	0.140
N3	16.96	12.00	16.26	2.62	2.07	0.142
N4	17.09	12.09	16.35	2.62	2.09	0.133
N5	17.14	12.12	16.52	2.62	2.08	0.135
N6	16.63	11.76	16.00	2.62	2.10	0.130
N7	16.87	11.93	16.19	2.62	2.07	0.131
N8	16.98	12.00	16.33	2.62	2.07	0.134
N9	17.08	12.07	16.37	2.62	2.07	0.137
N10	17.04	12.05	16.34	2.62	2.06	0.129
N11	17.73	12.53	16.99	2.62	2.07	0.127
N12	18.18	12.85	17.52	2.62	2.09	0.132
N13	18.46	13.06	17.64	2.62	2.03	0.132
N14	18.52	13.10	17.85	2.62	2.04	0.141
N15	18.56	13.12	17.85	2.62	2.03	0.139
N16	18.51	13.09	17.75	2.62	2.06	0.129
N17	18.30	12.94	17.45	2.62	2.03	0.125
N18	18.49	13.07	17.75	2.62	2.08	0.133
N19	18.44	13.04	17.73	2.62	2.04	0.137
N20	18.42	13.03	17.57	2.62	2.01	0.131
Average	**17.65**	**12.48**	**16.94**	**2.62**	**2.06**	**0.133**

Table A.7: Mean free-surface elevation $\bar{\eta}$ (cm) at seven wave gauge locations

Run	WG1	WG2	WG3	WG4	WG5	WG6	WG7
N1	-0.15	-0.15	-0.19	-0.03	0.35	0.43	0.58
N2	-0.17	-0.19	-0.17	-0.03	0.38	0.44	0.61
N3	-0.14	-0.13	-0.19	0.00	0.37	0.46	0.60
N4	-0.14	-0.13	-0.18	-0.02	0.38	0.46	0.57
N5	-0.14	-0.14	-0.19	-0.01	0.37	0.48	0.62
N6	-0.14	-0.12	-0.19	-0.04	0.34	0.41	NR
N7	-0.16	-0.14	-0.21	-0.03	0.36	0.43	0.52
N8	-0.14	-0.18	-0.17	-0.01	0.38	0.46	0.47
N9	-0.18	-0.15	-0.19	-0.02	0.36	0.44	0.57
N10	-0.14	-0.14	-0.18	0.01	0.39	0.48	0.66
N11	-0.09	-0.14	-0.20	-0.05	0.36	0.51	0.64
N12	-0.18	-0.24	-0.24	0.00	0.42	0.52	0.61
N13	-0.17	-0.14	-0.18	0.00	0.40	0.50	0.66
N14	-0.14	-0.16	-0.18	0.02	0.45	0.50	0.80
N15	-0.15	-0.15	-0.17	0.02	0.46	0.54	0.65
N16	-0.18	-0.18	-0.18	0.03	0.45	0.56	0.81
N17	-0.11	-0.13	-0.17	0.02	0.43	0.52	NR
N18	-0.12	-0.24	-0.19	0.02	0.42	0.48	0.73
N19	-0.15	-0.13	-0.18	0.04	0.45	0.54	0.73
N20	-0.12	-0.14	-0.17	0.03	0.44	0.52	0.66
Average	**-0.15**	**-0.16**	**-0.19**	**0.00**	**0.40**	**0.48**	**0.64**

NR implies "Not Reliable" data

Table A.8: Free-surface standard deviation σ_η (cm) at seven wave gauge locations

Run	WG1	WG2	WG3	WG4	WG5	WG6	WG7
N1	4.05	4.07	4.15	3.48	2.33	2.07	1.81
N2	4.08	4.08	4.16	3.48	2.33	2.05	1.81
N3	4.09	4.11	4.18	3.50	2.34	2.07	1.82
N4	4.13	4.15	4.22	3.50	2.34	2.07	1.82
N5	4.14	4.16	4.22	3.49	2.35	2.07	1.83
N6	4.02	4.02	4.12	3.41	2.35	2.06	1.69
N7	4.08	4.10	4.15	3.45	2.35	2.07	1.68
N8	4.10	4.12	4.18	3.45	2.36	2.07	1.69
N9	4.13	4.15	4.20	3.45	2.37	2.07	1.68
N10	4.13	4.15	4.20	3.48	2.37	2.07	1.71
N11	4.33	4.40	4.28	3.85	2.62	2.28	1.53
N12	4.45	4.52	4.38	3.88	2.65	2.30	1.54
N13	4.52	4.59	4.44	3.88	2.65	2.29	1.51
N14	4.53	4.60	4.45	3.91	2.65	2.28	1.53
N15	NA	4.61	4.46	3.89	2.66	2.30	1.50
N16	4.54	4.60	4.46	3.90	2.66	2.29	1.50
N17	4.48	4.55	4.42	3.85	2.64	2.30	1.94
N18	4.53	4.59	4.44	3.85	2.66	2.30	1.96
N19	4.51	4.59	4.44	3.86	2.66	2.30	2.03
N20	4.51	4.59	4.43	3.85	2.65	2.28	2.06
Average	**4.28**	**4.34**	**4.30**	**3.67**	**2.50**	**2.18**	**1.73**

Table A.9: Wet probability P_w, its mean free-surface elevation $\bar{\eta}$ (cm) and free-surface standard deviation σ_η (cm) for WG8

Run	t (s)	P_w	Z_b (cm)	$\bar{h}$ (cm)	$\bar{\eta}$ (cm)	σ_η (cm)
	0		9.01			
N1	200	0.29	9.04	1.43	10.47	0.68
N2	600	0.32	9.11	0.65	9.76	0.54
N3	1000	0.27	9.18	0.64	9.82	0.55
N4	1400	0.28	9.25	0.67	9.92	0.56
N5	1800	0.30	9.32	0.72	10.04	0.52
	2000		9.36			
N6	2200	0.28	9.42	1.34	10.76	0.55
N7	2600	0.29	9.54	0.71	10.25	0.53
N8	3000	0.25	9.66	0.71	10.37	0.57
N9	3400	0.26	9.78	0.65	10.43	0.56
N10	3800	0.26	9.90	0.68	10.58	0.56
	4000		9.96			
N11	4200	NR	9.98	NR	NR	NR
N12	4600	0.30	10.02	0.64	10.66	0.51
N13	5000	0.33	10.06	0.57	10.63	0.45
N14	5400	0.28	10.10	0.65	10.75	0.50
N15	5800	0.32	10.14	0.57	10.71	0.45
	6000		10.17			
N16	6200	0.29	10.19	0.62	10.81	0.45
N17	6600	0.29	10.23	0.64	10.87	0.45
N18	7000	0.32	10.27	0.51	10.78	0.43
N19	7400	0.23	10.31	0.63	10.94	0.48
N20	7800	0.31	10.35	0.55	10.90	0.46
	8000		10.38			
Average		**0.29**		**0.71**	**10.49**	**0.52**

* $t = 0$ is initial profile; $t = 4000$ is final profile. NR implies "not reliable" data

Table A.10: Mean cross-shore velocity $\bar{U}$ and standard deviation σ_U of the 2D ADV co-located with WG4 at $x = 8.30$ m, Red Vectrino co-located with WG5 at $x = 12.90$ m and Blue Vectrino co-located with WG6 at $x = 15.52$ m

Run	2D ADV at WG4		Red Vectrino at WG5		Blue Vectrino at WG6	
	$\bar{U}$ (*cm/s*)	σ_U (*cm/s*)	$\bar{U}$ (*cm/s*)	σ_U (*cm/s*)	$\bar{U}$ (*cm/s*)	σ_U (*cm/s*)
N1	-8.86	22.62	-3.11	14.61	-3.82	15.73
N2	-8.48	22.61	-3.74	14.49	-3.80	15.76
N3	-7.67	22.56	-3.18	14.64	-3.80	15.82
N4	-7.85	22.64	-3.26	14.61	-4.22	15.73
N5	-7.95	22.56	-3.08	14.66	-4.24	15.88
N6	-7.83	22.64	-3.10	14.62	-3.60	15.89
N7	-7.88	22.54	-3.33	14.59	-3.99	15.83
N8	-8.08	23.01	-3.47	14.69	-3.99	15.82
N9	-8.10	22.50	-3.49	14.60	-3.70	15.94
N10	-7.79	22.66	-3.57	14.69	-4.24	15.68
N11	-7.19	21.67	-4.40	NR	-4.26	15.48
N12	-8.33	22.16	-2.92	14.61	-4.00	15.52
N13	-7.75	22.38	-3.19	14.55	-4.10	16.60
N14	-8.13	21.96	-3.33	14.64	NR	NR
N15	-8.15	22.22	-3.16	14.52	-4.38	15.81
N16	-8.06	22.25	-2.97	14.63	-3.72	15.79
N17	-8.20	22.33	-2.86	14.70	-3.78	15.95
N18	-7.97	22.00	-2.82	14.44	-4.18	15.90
N19	-7.63	22.09	-3.10	14.63	-4.08	15.72
N20	-8.06	22.10	NA	NA	NA	NA
Average	**-8.00**	**22.38**	**-3.27**	**14.61**	**-3.99**	**15.83**

NA implies "not available" data
NR implies "Not Reliable" data

A.3 Positive (P) Net Cross-shore Sediment Transport Test

Figure A.13: Wave overtopping and overwash

Figure A.14: Beach profiles during run P1 and run P10 for positive net cross-shore
sediment transport test with water depth of 92 cm
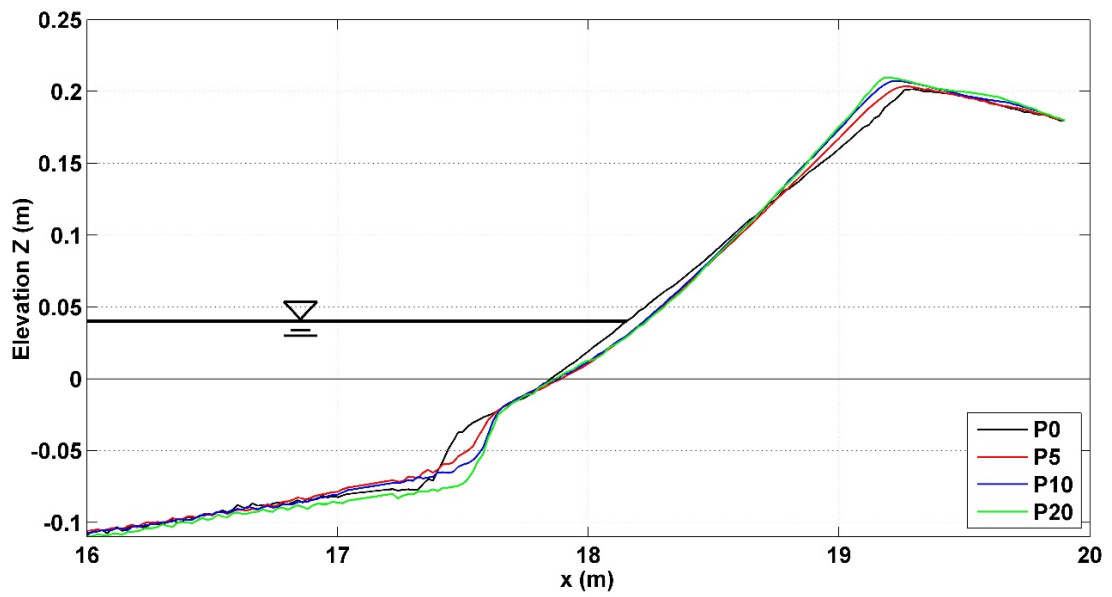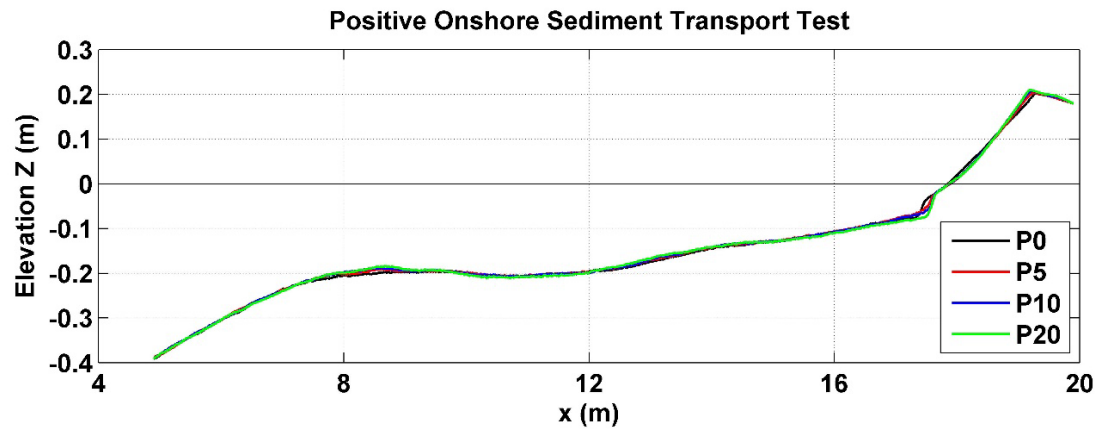
Figure A.15: Positive (P) net cross-shore sediment transport test with 20 runs where the still water level is located at the elevation of z=0.04m

Table A.11: Incident wave characteristics for Test P

Run	H_{mo} (cm)	H_{rms} (cm)	H_s (cm)	T_p (s)	T_s (s)	R
P1	17.73	12.53	17.00	2.62	2.10	0.142
P2	17.92	12.67	17.15	2.62	2.07	0.137
P3	18.06	12.77	17.30	2.62	2.06	0.143
P4	18.13	12.82	17.40	2.62	2.07	0.142
P5	18.11	12.81	17.32	2.62	2.07	0.144
P6	17.76	12.56	17.03	2.62	2.08	0.145
P7	17.95	12.69	17.10	2.62	2.05	0.140
P8	18.01	12.73	17.24	2.62	2.08	0.144
P9	18.11	12.80	17.41	2.62	2.07	0.147
P10	18.15	12.83	17.45	2.62	2.07	0.150
P11	17.74	12.54	17.04	2.62	2.09	0.145
P12	17.98	12.71	17.07	2.62	2.06	0.143
P13	18.11	12.81	17.42	2.62	2.06	0.149
P14	18.20	12.87	17.55	2.62	2.07	0.144
P15	18.16	12.84	17.58	2.62	2.05	0.148
P16	18.18	12.86	17.45	2.62	2.06	0.149
P17	18.18	12.85	17.53	2.62	2.05	0.151
P18	18.16	12.84	17.42	2.62	2.07	0.153
P19	18.34	12.97	17.63	2.62	2.06	0.147
P20	18.29	12.93	17.51	2.62	2.03	0.147
Average	**18.06**	**12.77**	**17.33**	**2.62**	**2.07**	**0.146**

Table A.12: Mean free-surface elevation $\bar{\eta}$ (cm) at seven wave gauge locations

Run	WG1	WG2	WG3	WG4	WG5	WG6	WG7
P1	-0.09	-0.13	-0.10	-0.10	0.22	0.20	0.34
P2	-0.10	-0.14	-0.07	-0.12	0.22	0.27	0.35
P3	-0.13	-0.14	-0.07	-0.14	0.22	0.27	0.33
P4	-0.12	-0.14	-0.07	-0.11	0.21	0.24	0.33
P5	-0.09	-0.14	-0.07	-0.10	0.23	0.28	0.32
P6	-0.08	-0.09	-0.08	-0.09	0.23	0.25	0.36
P7	-0.11	-0.12	-0.07	-0.15	0.25	0.24	0.33
P8	-0.08	-0.15	-0.07	-0.12	0.23	0.30	0.34
P9	-0.11	-0.12	-0.07	-0.13	0.24	0.30	0.36
P10	-0.10	-0.13	-0.07	-0.12	0.24	0.31	0.55
P11	-0.09	-0.12	-0.11	-0.13	0.18	0.23	0.30
P12	-0.18	-0.13	-0.08	-0.12	0.22	0.26	0.46
P13	-0.10	-0.15	-0.07	-0.13	0.23	0.32	0.36
P14	-0.09	-0.12	-0.08	-0.15	0.25	0.33	0.33
P15	-0.12	-0.13	-0.07	-0.12	0.24	0.29	0.33
P16	-0.13	-0.13	-0.07	-0.15	0.24	0.30	0.38
P17	-0.09	-0.13	-0.07	-0.14	0.26	0.26	0.36
P18	-0.11	-0.15	-0.07	-0.12	0.22	0.29	0.32
P19	-0.17	-0.14	-0.08	-0.15	0.26	0.31	0.37
P20	-0.12	-0.15	-0.07	-0.12	0.25	0.32	0.37
Average	**-0.11**	**-0.13**	**-0.08**	**-0.13**	**0.23**	**0.28**	**0.36**

Table A.13: Free-surface standard deviation σ_η (cm) at seven wave gauge locations

Run	WG1	WG2	WG3	WG4	WG5	WG6	WG7
P1	4.32	4.32	4.36	3.99	2.94	2.68	2.44
P2	4.38	4.38	4.42	4.01	2.98	2.71	2.46
P3	4.42	4.41	4.44	4.03	2.97	2.72	2.47
P4	4.44	4.44	4.45	4.04	3.00	2.72	2.47
P5	4.43	4.44	4.46	4.03	2.98	2.71	2.49
P6	4.35	4.34	4.35	4.01	2.95	2.70	2.47
P7	4.40	4.39	4.41	4.00	2.98	2.70	2.48
P8	4.42	4.41	4.41	4.05	2.98	2.72	2.47
P9	4.46	4.44	4.43	4.06	2.97	2.73	2.49
P10	4.46	4.45	4.44	4.08	2.97	2.73	2.65
P11	4.37	4.33	4.36	4.05	2.96	2.69	2.47
P12	4.44	4.39	4.41	4.06	2.97	2.68	2.46
P13	4.47	4.42	4.45	4.10	2.97	2.68	2.47
P14	4.49	4.45	4.48	4.11	2.96	2.68	2.46
P15	4.47	4.45	4.47	4.11	2.97	2.65	2.44
P16	4.47	4.46	4.46	4.13	2.96	2.67	2.44
P17	4.48	4.45	4.46	4.14	2.97	2.66	2.42
P18	4.47	4.44	4.46	4.10	2.97	2.64	2.42
P19	4.51	4.49	4.51	4.13	2.98	2.64	2.43
P20	4.51	4.48	4.49	4.11	2.96	2.65	2.43
Average	**4.44**	**4.42**	**4.44**	**4.07**	**2.97**	**2.69**	**2.47**

Table A.14: Wet probability P_w, its mean free-surface elevation $\bar{\eta}$ (cm) and free-surface standard deviation σ_η (cm) for WG8

Run	t (s)	P_w	Z_b (cm)	$\bar{h}$ (cm)	$\bar{\eta}$ (cm)	σ_η (cm)
	0		10.38			
P1	200	0.62	10.33	1.71	12.04	0.99
P2	600	0.63	10.24	1.45	11.69	1.03
P3	1000	0.62	10.16	1.45	11.61	1.03
P4	1400	0.64	10.07	1.52	11.59	1.07
P5	1800	0.65	9.98	1.42	11.40	1.08
	2000		9.94			
P6	2200	0.66	9.96	2.09	12.05	1.06
P7	2600	0.65	10.00	1.79	11.79	1.05
P8	3000	0.65	10.05	1.52	11.57	1.07
P9	3400	0.63	10.10	1.61	11.71	1.06
P10	3800	0.63	10.14	1.66	11.80	1.24
	4000		10.17			
P11	4200	0.61	10.16	2.28	12.44	1.05
P12	4600	0.61	10.15	1.51	11.66	1.06
P13	5000	0.64	10.15	1.53	11.68	1.06
P14	5400	0.62	10.14	1.57	11.71	1.06
P15	5800	0.61	10.13	1.63	11.76	1.06
	6000		10.13			
P16	6200	0.63	10.12	1.58	11.70	1.07
P17	6600	0.60	10.11	1.63	11.74	1.07
P18	7000	0.61	10.11	1.57	11.68	1.08
P19	7400	0.62	10.10	1.68	11.78	1.07
P20	7800	0.60	10.09	1.53	11.62	1.08
	8000		10.09			
Average		**0.63**		**1.64**	**11.75**	**1.07**

Table A.15: Mean cross-shore velocity $\bar{U}$ and standard deviation σ_U of the 2D ADV co-located with WG4 at $x = 8.30$ m, Red Vectrino co-located with WG5 at $x = 12.90$ m and Blue Vectrino co-located with WG6 at $x = 15.52$ m

Run	2D ADV at WG4		Red Vectrino at WG5		Blue Vectrino at WG6	
	$\bar{U}$ (*cm/s*)	σ_U (*cm/s*)	U (*cm/s*)	σ_U (*cm/s*)	$\bar{U}$ (*cm/s*)	σ_U (*cm/s*)
P1	-7.68	22.08	-3.79	15.76	-3.29	17.18
P2	-7.87	22.39	-3.88	15.84	-3.36	17.28
P3	-8.16	22.46	-4.07	15.78	-4.19	17.11
P4	-7.85	22.53	-3.73	15.80	-3.88	17.27
P5	-8.49	22.83	-3.89	15.89	-3.61	17.31
P6	-7.54	21.78	-3.90	16.09	-3.88	17.20
P7	-8.24	22.37	-3.80	15.89	-3.66	17.18
P8	-8.00	23.08	NA	NA	NA	NA
P9	-7.41	22.81	-3.67	15.92	NR	NR
P10	-8.66	22.80	-3.32	15.95	-3.48	17.17
P11	-7.94	22.60	-3.76	15.87	-3.39	17.22
P12	-8.37	22.85	NA	NA	NA	NA
P13	-8.91	22.53	-3.92	15.75	-3.38	17.15
P14	-8.04	22.96	-4.24	15.77	-3.24	16.99
P15	-8.12	22.65	-4.14	15.80	-3.15	16.85
P16	-8.10	22.70	-4.21	15.81	-3.62	16.85
P17	-8.14	22.70	NR	NR	-3.14	16.95
P18	-7.99	22.52	-4.19	15.74	-3.27	16.89
P19	-7.62	22.77	NR	NR	-3.79	16.99
P20	-7.89	22.85	-4.05	15.85	-3.63	16.87
Average	**-8.05**	**22.61**	**-3.91**	**15.84**	**-3.53**	**17.09**

NA implies "not available" data
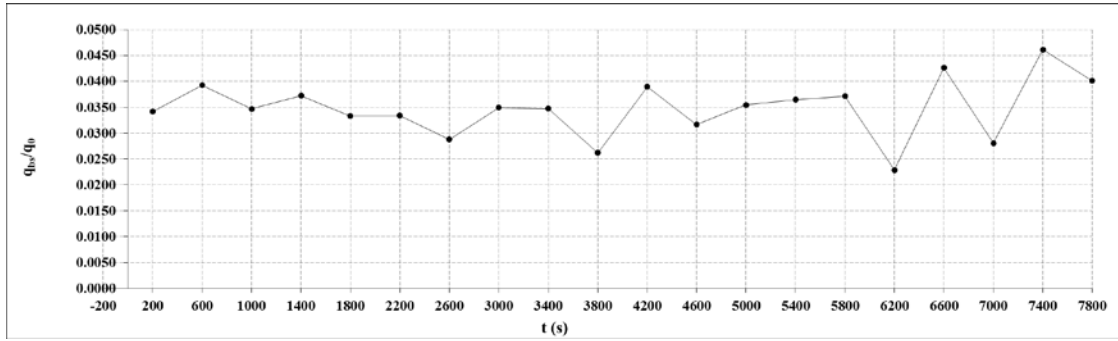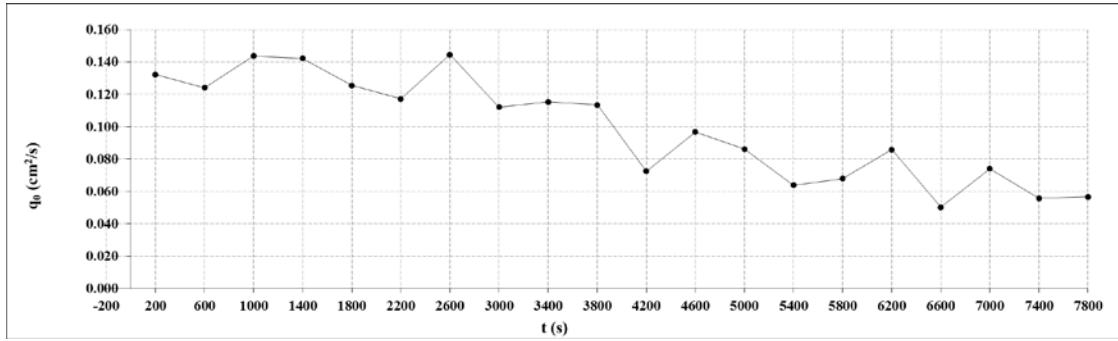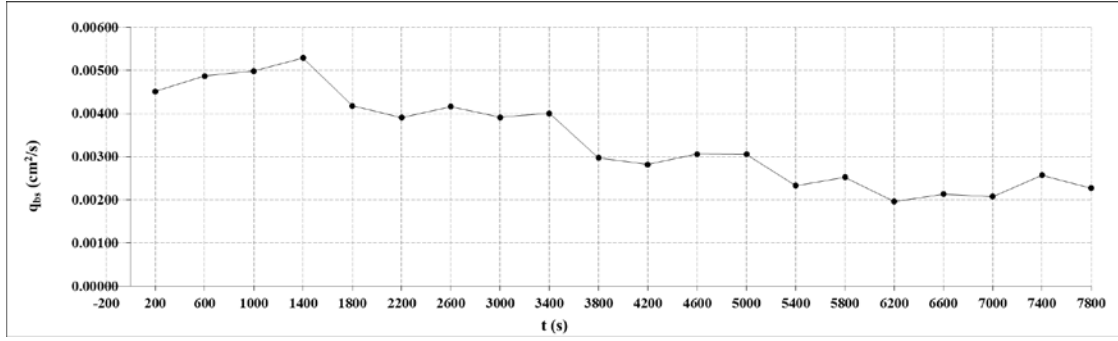*NR implies "not reliable" data*

Figure A.16: Temporal variation of sand overwash rate q_{bs} (top), wave overtopping rate q_o (middle) and their ratio q_{bs}/q_o (bottom)